Development and Optimization of High-throughput Zebrafish Screening Platform

MASSACHUSETTS INSTITUTE OF TECHNOLOGY
SEP 2 9 2010
LIBRARIES

ARCHIVES

by

Bryan Kyo Koo

B.S. in Electrical Engineering and Computer Science

Massachusetts Institute of Technology, 2009

SUBMITTED TO THE DEPARTMENT OF ELECTRICAL ENGINEERING AND COMPUTER SCIENCE
IN PARTIAL FULFILLMENT OF THE REQUIREMENT OF DEGREE OF

MASTER OF ENGINEERING IN ELECTRICAL ENGINEERING AND COMPUTER SCIENCE

AT THE MASSACHUSETTS INSTITUTE OF TECHNOLOGY

May 2010
[June 2010]

© 2010 Bryan Kyo Koo. All Rights Reserved.

The author hereby grants to MIT permission to reproduce and
to distribute publicly paper and electronic copies of this thesis document in
whole or in part in any medium now known or hereafter created.

Signature of Author: _____
Department of Electrical Engineering and Computer Science
May, 2010

Certified by: _____
Mehmet Fatih Yanik
Professor of Electrical Engineering and Computer Science
Thesis Supervisor

Accepted by: _____
Christopher J. Terman
Professor of Electrical Engineering and Computer Science
Chairman, Department Committee on Graduate Theses

Development and Optimization of High-throughput Zebrafish Screening Platform

by

Bryan Kyo Koo

Submitted to the Department of Electrical Engineering and Computer Science
on May, 2010 in Partial Fulfillment of the Requirements for the Degree of
Master of Engineering in Electrical Engineering and Computer Science

ABSTRACT

The high-throughput zebrafish screening platform is a revolutionary tool that enables subcellular precision *in vivo* whole animal screening of Danio Rerio. It can perform laser surgery and/or imaging in less than twenty seconds per fish. This is a two orders of magnitude improvement from the existing manual method, which takes 10 to 15 minutes per fish. The platform also has the ability to rotate the fish in any angle for imaging or laser surgery. There has never been a platform that could align and position a zebrafish consistently and efficiently in such manner before. This crucial functionality was realized through a design in which zebrafish was screened in a capillary tube.

Thesis Advisor: Mehmet Fatih Yanik
Title: Professor of Electrical Engineering and Computer Science

Table of Contents

1. Introduction 9
2. Background 11
   2.1 Zebrafish in Modern Research 11
   2.2 C. Elegans Whole-Animal In Vivo Screening 13
   2.3 Current and Past Zebrafish In Vivo Screening 14
   2.4 Capillary for Ideal Microscopy 15
3. Microfluidic Chip Method 17
   3.1. Building Microfluidic Chips 17
      3.1.1 AutoCad 17
      3.1.2 DXF2G-Code 18
      3.1.3 G-Code Manipulation 19
      3.1.4 Fabrication 20
   3.2 Microfluidic Chip Designs 21
      3.2.1Early Stage Design 21
      3.2.2 Mid Stage Design 23
      3.2.3 Last Stage Design 24
4. Design of the High-throughput Screening Platform 27
   4.1 Hardware Components 27
      4.1.1 Photodetector Unit 28
      4.1.2 Objective Cage Unit 34
      4.1.2 Multiwell Plate Stage 37
      4.1.4 Syringe Pump 40
      4.1.5 Pinch Valves 41
   4.2 Software Components 42
      4.2.1 Syringe Pump Control 42
      4.2.2 Motor Control 45
      4.2.3 Multiwell Stage Control 48
      4.2.4 Camera & Machine Vision 49
      4.2.5 Overall Control of the Platform 50
5. Platform Performance Testing 53
   5.1 Health Assessment 53

5.1.1 Swimming Bladder 53
5.1.2 Assessment Method 54
5.1.3 Assessment Result 56
5.2 Speed Measurement of Individual Parts of the System 57
5.2.1 Assessment Method 58
5.2.2 Assessment Result 58
6. Imaging Capability of the Platform 60
7. Future Work and Improvement 62
7.1 Confocal Imaging 62
7.2 Pipelined Screening 64
7.3 Ultrathin Borosilicate Capillary 65
8. Summary 66
9. Bibliography 67

Table of Figures

Figure 1 Side-view of 2-day old Zebrafish 11

Figure 2 C. Elegans (left) and Zebrafish (right) under flourescent light. C. Elegans have fewer marked neurons that are more visible. The main neurons are harder to view in zebrafish due to flouresence noise from minor neurons 14

Figure 3 The Matlab interface of dxf2gcode. Top right window is Figure 1: GUI for manually selecting paths. Left window is Figure 2: a log of G-code converted thus far. Bottom right window is a 3-d diagram of G-code that has been converted thus far. 18

Figure 4 One of the early chip designs. The red paths indicate the order that zebrafish navigates through the chip. The triangular structure on top right is the isolation chamber and the trapezoidal structure on the left is the immobilization chamber 21

Figure 5 One of the mid-stage designs. Isolation chamber is the same as the design in Figure 4. However, the immobilization chamber has been modified in this version 23

Figure 6 Zebrafish immobilized imperfectly in the chamber. Notice the depression layer not quite pressed on the right side near the fish's head. This chamber was also too large. 24

Figure 7 One of the late-stage designs. The immobilization chamber on the left is sloped towards the bottom of the chip. The inlet and outlet channels funnel out. 25

Figure 8 Zebrafish trapped in the immobilization chamber of chip design in figure 7. Zebrafish is trapped at the deeper part of the chamber after the immobilization layer depressed on it. The fish in this picture is older and bigger than the ones that are commonly used for screening, which is why it does not quite fit in the chamber. 26

Figure 9 Schematic Diagram of the Platform 28

Figure 10 The Signal Logic for the Photodetector Unit. The first peak represents the signal from an air bubble, and the second peak represents the signal from a zebrafish. You see that with the two signals combined, zebrafish's signal has a bigger magnitude. 31

Figure 11 The picture (left) and the input/output diagram of OPT301 Photodiode Integrated Circuit 32

Figure 12 The inner circuitry of OPT301 33

Figure 13 Circuit Design of the Photodetector unit. It is connected to four Nidaq ports. Note that the two LED's are integrated on the same board 33

Figure 14 Diagram of Photodetector Unit. Green LED is shone right through the capillary on the photodiode, and the blue LED is shone perpendicular to the green light. Paths of light are all contained within the black polyurethane block 34

Figure 15 Photo of Jameco Stepper Motor 36

Figure 16 Photo of Interinar BSD-02LH Motor Controller. The black socket with ten gold pins is where a rainbow cable can be plugged in. However, the wires can also be connected individual through the green screw-in ports on bottome left and top left of the picture. The four ports on the top right are the ports where the four lead wires from bipolar stepper motor connects. 37

Figure 17 Photo of Prior H101A Stage. 39

Figure 18 Diagram of Fish Loader/Dispenser in conjunction with one of the 96 wells on a plate. The narrower tip acts as an outlet to prevent pressure build-up during aspiration or dispensation... 40

Figure 19 Photo of Tricontinent C3000 Precision Syringe Pump 41

Figure 20 Photo of Biochem-Valve 075P2NC12-02SQ Pinch Valve 41

Figure 21 Photo of Biochem-Valve 075P2NC12-02SQ Pinch Valve 42

Figure 22 The diagram of the 10-pin connection of Interinar BSD-02LH Motor Controller 46

Figure 23 Schematic Diagram of the screening platform. V1,V2,V3 are the pinch valves that function as the logic gates of the screening process. 51

Figure 24 GUI for the screening platform. (Left) Syringe GUI (Right top) Motor GUI (Right bottom) Multiwell GUI 52

Figure 25 Zebrafish with fully-developed swimming bladders (right) and with underdeveloped swimming bladders (left) 54

Figure 26 Zebrafish with edema. Internal organs, especially the yolk sack is more opaque and the chest cavity containing the heart is severely enlarged 55

Figure 27 Number of zebrafish larvae with fully developed swimming bladders after going through the system at 200/400/200, 300/400/300, 400/400/400, respectively 56

Figure 28 Number of zebrafish larvae with fully developed swimming bladders between the control group and the group that went through the system at 400/400/400 speed 57

Figure 29 The images of wild type zebrafish (left) and astray zebrafish (right). The neuronal paths on the left form a clear X, whereas the ones on the right are randomly scattered from the brain to the eyes. 61

Figure 30 Digitally reconstructed image of confocal microscopic scans of zebrafish's head with fluorescence in its vasculature. (Weistein Laboratory, NIH) 63

Figure 31 Tentative Schematic Diagram of the pipelined high-throughput screening platform. It operates with three syringe pumps and two multiwell plate stages. 64

Table of Tables

Table 1 Attributes of some key animals used to model human disease. -, not relevant, or not a strength; $, $$, $$$ and +, ++, +++, relative cost ($) and strength (+) of the model in each category 13

Table 2 List of Material used to build capillaries in optical and biological applications 15

Table 3 The functionalities of the 10-pin connection of the motor controller 46

Table 4 The microstep sizes based on the states of MS1 and MS2 47

Table 5 The average time spent per section of the platform and its standard deviation 58

1. Introduction

My thesis work was part of a larger project to develop a high-throughput whole-animal bioscreening platform for zebrafish larvae at Professor Yanik's High-Throughput Neurotechnology Group in Massachusetts Institute of Technology Research Laboratory of Electronics. We aspired to create a platform that enables a high-throughput screening of zebrafish larvae in the order of one screen per 20 seconds, which is two orders of magnitude faster than the existing manual method, which is in between 15-20 minutes. We employed devices such as photodiode, computer controlled syringe pump, step motor. The computer interface was implemented in Matlab while the image capturing was done through the proprietary software provided by the camera itself. The project was targeted especially to the field of bio and neuronal research usage, because the completed platform could facilitate zebrafish screening in the volume unimaginable in the past.

The project was first incepted in the summer of 2008 by a summer researcher Hasan Celiker and a graduate student Cody Gilleland. The initial goal was to take the approach and methods of the C. Elegans project within the lab headed by Chris Rohde and Cody, and apply it directly to zebrafish. The project was then put on halt after the summer until I came under Cody's supervision for the project during January of 2009. We continued the approach of imaging zebrafish in a microfluidic chip with until we decided that it would be more efficient and accurate to image the fish in a capillary tube. Afterwards, graduate students Carlos Pardo and Michael Chang took over the project on the summer of 2009 along with me. We also started seeking advice and supervision from a Bioengineering Department instructor, Steven Wasserman. There were also five additional researchers onboard for the summer who assisted in the development of the prototypes for the platform, management of the zebrafish, and experimenting with alternative data acquisition methods. The project, which continued with Carlos, Mike, and I, culminated in a paper titled *High-throughput subcellular-resolution in vivo vertebrate screening platform* that was submitted to Nature Methods on January 8th, 2010.

My role in the project before the change to capillary was to design and fabricate microfluidic chips. During the summer of 2009, I became responsible for a segment of the project that included more diverse tasks. First, I was in charge of finding an appropriate capillary for the zebrafish to be imaged in instead of microfluidic chip. I was also in charge of designing and building a stepper motor system that would rotate the capillary under the objective both on software and hardware side with Carlos. Learning and interfacing the syringe pump for the entire system was a task shared with Michael. Michael and I also developed the photodetector system, along with a few other components to the mechanical and fluidic aspects of the system. I was not involved with the selection and set up of the microscopes, laser, and the major decisions in which strains of zebrafish and assays to be used with the platform. I only observed and assisted in the actualization of the imaging part of the platform, but I did have a major role in testing and optimizing the mechanical controls.

In this thesis report, I first introduce some of the background material on the field of whole animal bioscreening and factors that played major roles in making decisions for the project. As a part of that effort, I give an overview of the microfluidic approach of the project. Then I describe the hardware and software design for the system excluding the microscopy aspect of it. The result section is divided into two sections, first being the performance test including the health assessment and the speed measurement, and second being the demonstration of imaging capability of the platform with images taken during screening. Future works and improvements outline the work that has been done from January until May, and also other modifications and improvements that are in plans for the platform. After the summary, appendices include basic knowledge and mechanism of the devices or software used in the platform.

2. Background

2.1 Zebrafish in Modern Research

Zebrafish, binomial name Danio Rerio, is an important model organism for vertebrae development and gene function research. The value of zebrafish as a model for human disease has been substantiated by multiple recent publications that described of zebrafish mutations with diseases characteristic to humans. There is a rich set of genetic tools that are capable of locally modifying zebrafish gene to create mutations in various functions in the body, including the liver, eyes, the central nervous system, heart, and even blood. These genetic tools are only multiplying in numbers and as a result, zebrafish, which was initially envisioned as a model simply to bridge the gap between C elegans and lab rats, turned out to be a valuable model in its own right.[1]

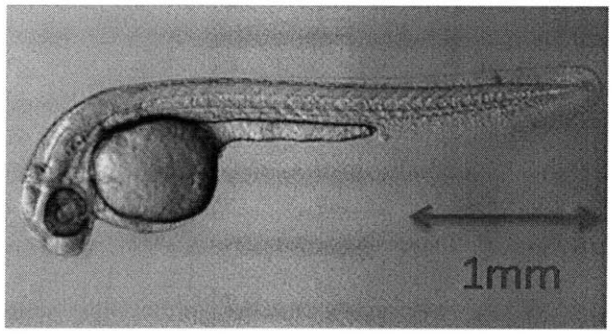

Figure 1 Side-view of 2-day old Zebrafish.

Apart from its value as a model organism close to humans, zebrafish has many traits that make it very a convenient and useful for research. Its embryo develops rapidly, progressing from egg to larva in less than three days. It also takes only three months for the embryos to mature enough to procreate. The embryos are large, robust, and transparent, so are the larvae for the first 7 days of their life. They develop externally to the mother.[2] All these characteristics facilitate easier experimental manipulation and observation than other common vertebrae model organism such as rattus norvegicus. Especially the

[1] Barut
[2] Kimmel

transparency of larvae is unforeseen characteristic in any other vertebrae model organism. Furthermore, zebrafish is currently the only vertebrae model organism in millimeter scale used for bio research. It develops physiological traits such as the nervous system, circulatory system, and digestive systems that also exist in human bodies, yet it is several magnitudes of order smaller than rattus norvegicus in size and maturity rate.

A great merit of small organisms such as zebrafish and C. elegans is that only in their size is it possible to do a whole-animal screening with the entire organs and tissues under the microscope. There have been a plethora of these two model organisms with specific organs, neurons, and tissues marked with fluorescence dye. This enables a very accurate and clear imaging of those organs, which can be observed for mutation, deterioration, regenerations, and etc.

The maintenance of zebrafish is also more cost and space efficient than other model organisms. Zebrafish facilities can grow 25-30 adult zebrafish in a cubic foot space in which only one to two lab rats can be grown. The fish only need to be fed twice a day to grow healthily. Each zebrafish can be mated as often as twice a week, producing 200-300 eggs per time. This is two orders of magnitude higher than rats, which only produce 15-20 pups per litter every month. Therefore, zebrafish can be used to screen assays in the scale unimaginable for rats due to the drastic difference in throughput. C. elegans share these merits in terms of throughput and volume, but the organism is far too removed from humans genetically and physiologically to do any reliable biomedical assay screening. Zebrafish is a very efficient organism to test assays before moving onto rat testing, since the latter takes much more resources and time.

It is difficult to find comparisons between the three organisms mentioned here (C. elegans, rats, and zebrafish) all together since C. elegans are drastically different from rats and zebrafish in many aspects, but there is a table of comparison among some of the model organisms in terms of their cost and their biological significance as a model organism published by Nature Review, part of which is listed on Table 1.

Attribute of Disease Model	Model Organism			
Practical Issues	Fly	Zebrafish	Mouse	Rat
Husbandry Infrastructure	$	$	$$$	$$$
Cost Per Animal Per year	$	$	$$$	$$$
Characterized Inbred Strains	+	-	++++	+++
Outbred Laboratory Strains	+	+++	++	++
Anatomical Similarity	-	+	++	++
Molecular or Genetic Similarity	+	++	+++	+++
Pathological Similarity	-	++	+++	+++
Storage; For Example, Freezing Sperm	No	Yes	Yes	Yes

Table 1 Attributes of some key animals used to model human disease[3]. -, not relevant, or not a strength; $, $$, $$$ and +, ++, +++, relative cost ($) and strength (+) of the model in each category

2.2 C. Elegans Whole-Animal In Vivo Screening

The effort to achieve automated, high-throughput whole animal screening has only started in past few years. The objective of my project was achieved with C. Elegans at High-throughput Neurotechnology group by Zeng, Rohde, and Yanik whose work was published on *Sub-cellular Precision On-Chip Small-Animal Immobilization, Multi-Photon Imaging and Femtosecond-Laser Imaging and Femtosecond-Laser Manipulation*. They developed an automatic high-throughput screening system for C. elegans that was capable of sub-cellular precision surgery and imaging. The complete immobilization of C. elegans was achieved by using depressive layers on silicone microfluidic chips. The chip described in the paper is capable of drug screening, microsurgery, and imaging at an unforeseen rate through a 2-D design and a relatively simple control system.[4]

It later became apparent that some of the fundamental differences between the two organisms made the adaptation of technique unrealistic. C elegans' physiology is practically one dimensional, requiring no rotational alignment. Focusing on a target neuron is also much easier because the organism is thin and it only has a few major neuronal paths, so it leaves very little chance of having much noise in the image. Due to a more complex neural network, there are very few strains of

[3] Currie
[4] Zeng

zebrafish with fluorescence marks that just light up the few major neurons. Even in the latter case, it is often challenging to focus on the target neuron due to the thickness of the organism in comparison to the thickness of its neuron. C elegans are also much more resistant to physical pressure applied to them, whereas zebrafish is injured quite easily from the same depressive layers used to immobilize c elegans.

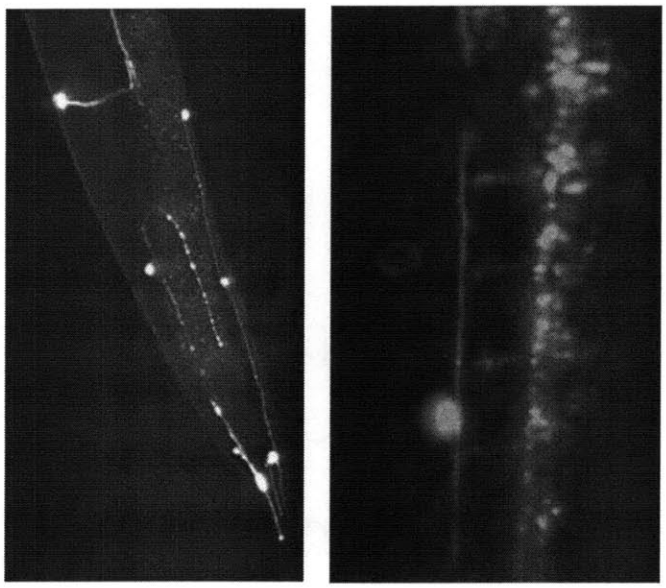

Figure 2 C. Elegans (left) and Zebrafish (right) under fluorescent light. C. Elegans have fewer marked neurons that are more visible. The main neurons are harder to view in zebrafish due to flouresence noise from minor neurons.

2.3 Current and Past Zebrafish In Vivo Screening

There have been several publications on in vivo screening of zebrafish with various methods and levels of success. Wang, Liu, and Sun from University of Toronto has devised a system where zebrafish embryos are immobilized in wells through suction and grown into larvae while immobilized.[5] Although this method insured an immobilization of individual zebrafish without notable damage to the organism, there is no control over which direction that the fish would grow to be. Moreover, the method itself is

[5] Wang

very limiting because the larva is always constrained in the well. It prohibits precise imaging or surgery and it is detrimental that the individual larva cannot be transported.

The one distinguishing characteristic of my thesis, which is imaging zebrafish larva in a capillary, has been implemented before by Funfak and Brosing as illustrated in *Micro fluid segment technique for screening and development studies*. In their set-up, zebrafish embryos are aspirated in Teflon capillary tubes and each of them occupies a section of medium that is separated within the tube by air bubbles. Embryos then grow to be larvae in this long string of medium.[6] However, this method is also severely limiting since the organism cannot be manipulated or screened with drugs once they are put in the capillary. Although this system used automatic syringe pump and Teflon tubes like my project, it did not utilize the merits of the respective elements as we did in our project.

2.4 Capillary for Ideal Microscopy

The process of selecting the right kind of capillary for imaging was not a trivial step. Initial idea of capillary imaging was tested with a borosilicate capillary tube and the bright-field imaging displayed a promising performance with a high-level of resolution. However the difference between refractory index of borosilicate glass and water (all the imaging in the project was done with water immersion lenses) caused the image to blur due to light scatter. It was discovered that Teflon polymers generally had a closer index of refraction to water as can be seen on table 2.

Material	Index of Refraction
Water (in 20 Celsius)	1.333
Borosilicate Glass	1.517
Quartz Glass	1.46
Teflon PTFE (Polytetrafluoroethylene)	1.35
Teflon FEP (Fluorinated Ethylene Propylene)	1.338

Table 2 List of Material used to build capillaries in optical and biological applications

[6] Funfak

Even among Teflon polymers, FEP had the closest index of refraction with a marginal difference of .005. There was some issue of autofluorescence in the material, since it wasn't completely clear, but it was the best among all the options due to its refractive index. The FEP capillaries were also easier to handle since unlike borosilicate ones, they were flexible. This also proved to be a good decision in the long run because we eventually will need to inject individual zebrafish with needles. This process would be possible with Teflon tubes that could be punctured without cracking due to its elasticity, but not with most glass. There was a possibility of using square borosilicate capillaries, which eliminated the need of matching index of refraction, but this option would have defeated the purpose of using capillary to begin with, which was to have the freedom of rotational imaging.

It should also be mentioned that imaging the fish through a gel was also considered. This method would have involved dropping the fish in a well filled with liquid form of agar gel and then mixing it with an agent to cure the liquid and solidifying it, resultantly trapping the fish inside. However, this method seemed highly unrealistic because the alignment would be even more difficult and cutting the fish from the oxygen source and encapsulating it in gel would most likely have negative influence on its health. Most importantly, the process of curing and thawing the gel themselves would take much longer than 20 seconds, defeating the main goal of the platform.

3. Microfluidic Chip Method

The initial high-throughput zebrafish screening platform prototypes relied on microfluidic chip for a long duration due to the success of the C. Elegans project. Using microfluidic chips had many merits in automated screening for C. Elegans because they could be manipulated in a small chamber with precise fluidic control and surface manipulation. However, even with these capabilities, zebrafish proved to be too delicate and sophisticated to be controlled with methods employed by the C. Elegans project. However, this is not to say that there is no hope in employing microfluidics to high-throughput zebrafish screening. With more precise 3-D fabrication and possibly different kinds of silicone, it could be possible to create a chip that could effectively screen zebrafish larvae.

3.1. Building Microfluidic Chips

3.1.1 AutoCad

All of the chip design for this project were done in computer-aided design (in short CAD) software AutoCad. Although the software had 3-D capabilities, most of the designs were done in 2-D, since most of the chips were made from flat drill paths. Selected few designs later on in the project did have z-coordinate gradients of drill. It should be noted that the design from AutoCad is only a collection of drill paths. Within AutoCad program, there is no functionality to dictate anything on the design but the 2-d display of lines the software. The decisions and calculations of what size drill would mill out which drill path all had to be measured and calculated alongside the design. Therefore, it is often helpful to engrave the basic specs within the design file itself to avoid confusion in fabrication if it is possible.

3.1.2 DXF2G-Code

Once a design is completed using AutoCad, the file has to be saved in a DXF format. Matlab script called dxf2gcode was used to convert the DXF files into a machine code called G-code. When the script is activated, one of the designs can be chosen to be converted to drill paths. Once a file is chosen, Matlab displays three screens as shown below. Figure 1 on top right displays the design and enables you to assign the origin of the path coordinates, the scale of the design, and the drill paths. Figure 2 on the left displays the actual G-code that specifies the drill path, and figure 3 on the bottom right displays the visual 3-d path of the design that has been converted to G-code.

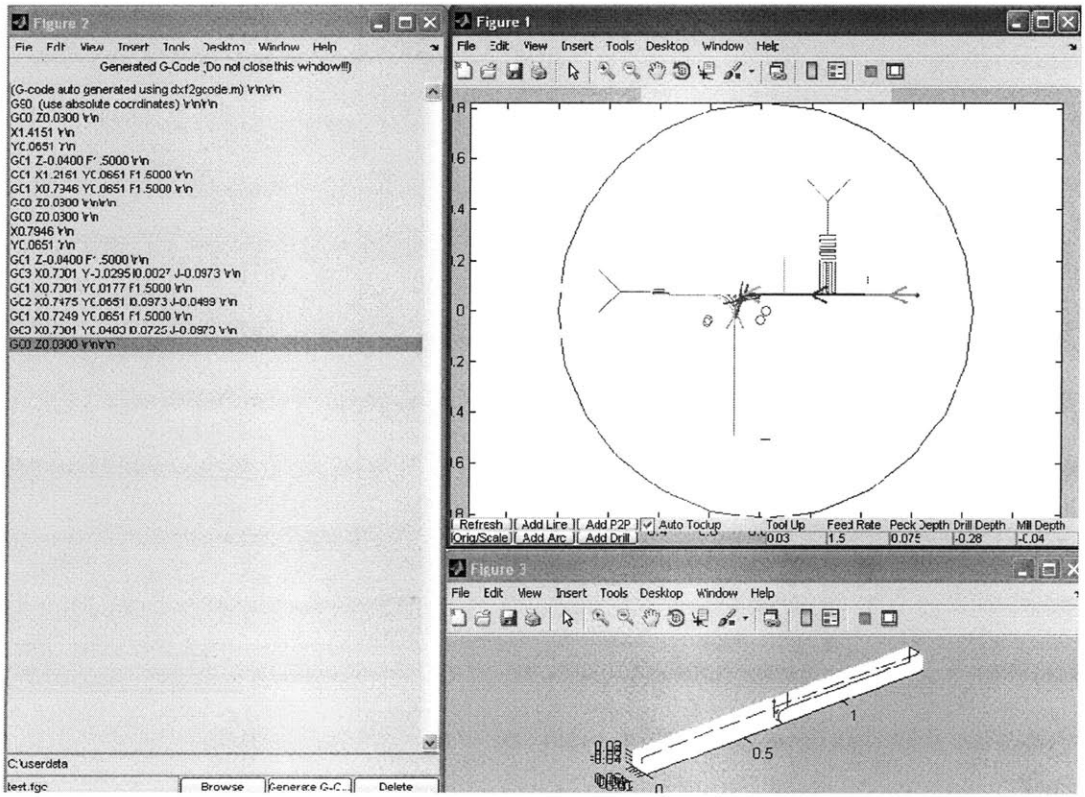

Figure 3 The Matlab interface of dxf2gcode. Top right window is Figure 1: GUI for manually selecting paths. Left window is Figure 2: a log of G-code converted thus far. Bottom right window is a 3-d diagram of G-code that has been converted thus far.

The first step in this procedure is to set the origin then choose a segment on the design to decide the scale. For this project, each chip design had a segment on the bottom that was .04 inch long

for the purpose of scaling only. This was important because the CNC machine used for the project ran on inch scale, and it was important to uniformly design and convert the drill paths in inches. Every time the lines on the design are converted to drill paths, the drill depth and the drill movement speed need to be chosen. Since each chip usually needs two to three different drill bits to mill out the path, separate G-codes were created for respective drill bit.

3.1.3 G-Code Manipulation

As noted in the previous section, all the AutoCad designs in this project were done in 2-d, and 3-d element was added directly to the G-code. Following is a sample G-code.

```
G00 Z0.0300
X0.3197
Y0.2231
G01 Z-0.1200 F1.5000
G01 X0.5197 Y0.2231 F1.5000
G01 X1.1197 Y0.2231 F1.5000
G01 X1.3197 Y0.2231 F1.5000
G00 Z0.0300
```

Outlining the first few steps of this code, the drill goes up by .03 (or move to z coordinate of .03) from wherever it was. Then it moves to x-coordinate of .3197 and y-coordinate of .2231. Afterward, it lowers the drill by .12 then move right to x=.5197 while staying on the same y-coordinate. Notice that the z-coordinate is not specified, because in G-code, unless noted, the z-coordinate stays the same from the previous location input.

It is actually possible to change the Z-coordinate within the same path. You can manually type in the z-coordinate since G-code is nothing more than a series of plain text. For example, if the drill needs to move up in Z-coordinate at a gradient of .06 inches at the either end of this path, following changes can be made.

```
G00 Z0.0300
X0.3197
Y0.2231
G01 Z-0.1200 F1.5000
G01 X0.5197 Y0.2231 Z-.06 F1.5000
G01 X1.1197 Y0.2231 F1.5000
G01 X1.3197 Y0.2231 Z-.12 F1.5000
G00 Z0.0300
```

Now the path is not on the same Z-plane, but instead the first and third paths are at a slope of .06 and -.06 respectively, outlining an isosceles trapezoidal path. Although occasionally time-consuming , for more elaborate changes, this method was chosen whenever there was a need to make a z-coordinate gradient on the chip design.

3.1.4 Fabrication

Fabrication refers to all the physical and chemical steps necessary to build a microfluidic chip. First, the G-code is transferred to the Computer Numerical Controlled (in short, CNC) station. The file is then opened in the CNC program that runs the milling machine. For each drill path of the chip, the correct drill bit is manually replaced on the machine before drilling on a polycarbonate plate. Once the polycarbonate plate is milled, the rough edges are smoothened out by carefully cutting off the remaining debris and cleaning the surface. Afterwards, the polycarbonate plate is vapor-polished with methylene chloride. Vapor polishing is executed by boiling the corrosive methylene chloride in a contained space and exposing the polycarbonate plate in the space to round out the channel and clear out the debris that are too small to be removed by corroding them with the methylene chloride fume. Following this, degassed polyurethane mixture is poured on the polycarbonate plate to create a black mold. It is then degassed again in a vacuum chamber to insure that there is no air bubble trapped in the liquid before it hardens. After the black mold is greased, polydimethylsiloxane (PDMS) is poured directly to create the microfluidic chips. The grease prevents the PDMS to get stuck to the surface, which can cause it to break. The pressure layer is fabricated on a separate crystal plate with multiple pressure layer patterns

by spin coating the wafer with PDMS to create a millimeter-thick membrane. The silicon chip and the pressure layer are bonded together by thermal bonding and then they are plasma-bonded in a vacuum on top of a glass slide. The reason that we bond it on glass instead of metal is to allow imaging through the plate.

3.2 Microfluidic Chip Designs

3.2.1 Early Stage Design

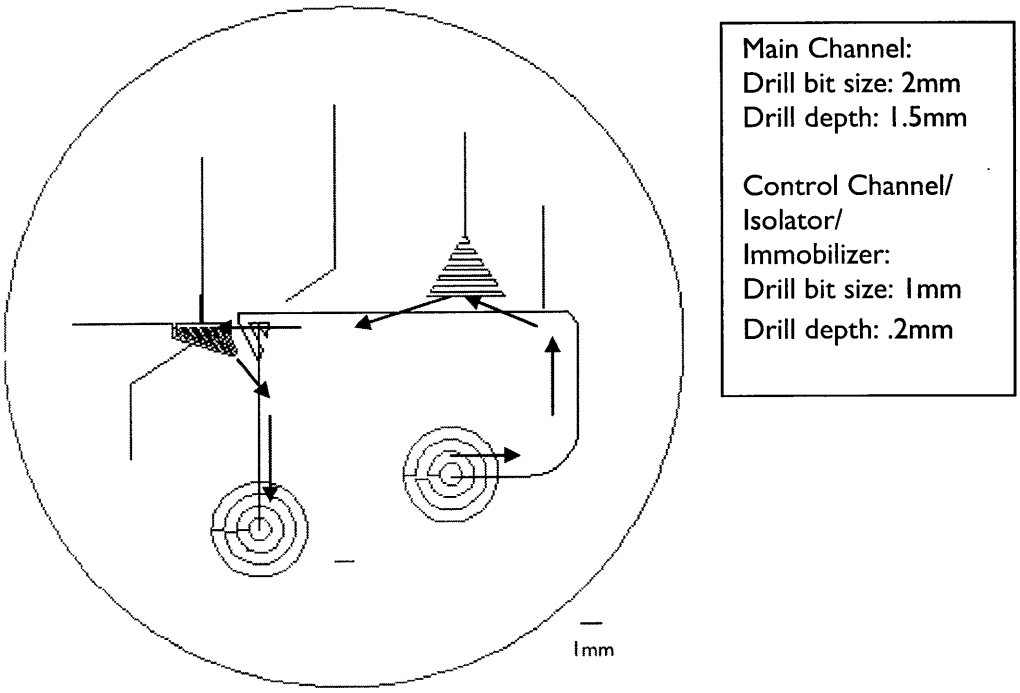

Figure 4 One of the early chip designs. The red paths indicate the order that zebrafish navigates through the chip. The triangular structure on top right is the isolation chamber and the trapezoidal structure on the left is the immobilization chamber.

First few microfluidic designs looked like Figure 4. The two concentric circles are the holes where syringe tips are positioned to let zebrafish in and out. The channel in blue is the main channel where the zebrafish travels down the chip. The purple lines on the periphery of the flow channel are the

control channels, which eject or absorb water to control the position of zebrafish in the chip. The control channels were milled out with drill bits small enough not to let any zebrafish body part through. The purple triangular region is an isolation chamber where the chip aspirates one zebrafish and let others go through the drain so the chip can insure that there is only one zebrafish in the chip. The trapezoidal chamber on the left is the immobilization chamber where it aspirates the zebrafish and presses down on it from the top with a depressive membrane. The red arrows on figure 3 indicate the path a zebrafish goes through in the chip during screening. It first enters the chip on the right bottom, then travels up the channel and gets isolated by the isolation chamber. Zebrafish is then pushed further left and is eventually pressed down in the immobilization chamber. After screening/surgery/imaging is done, the zebrafish exits the chip through the other circular hole in the bottom left.

This design had a few problems that needed to be improved.

1) The inlets and the outlets were designed so that they come in perpendicular to the chip, but this caused zebrafish to hit the bottom of the chip and die upon arrival.
2) All the channels were too big. The flow channels had too much unnecessary space and even the control channels were big enough to cause zebrafish get stuck in them.
3) The immobilization chamber did not work very well because it was too big. A simple pressure layer like the one in C. Elegans chip was not effective in holding the zebrafish in position since zebrafish is not flat or small like C. Elegans.

3.2.2 Mid Stage Design

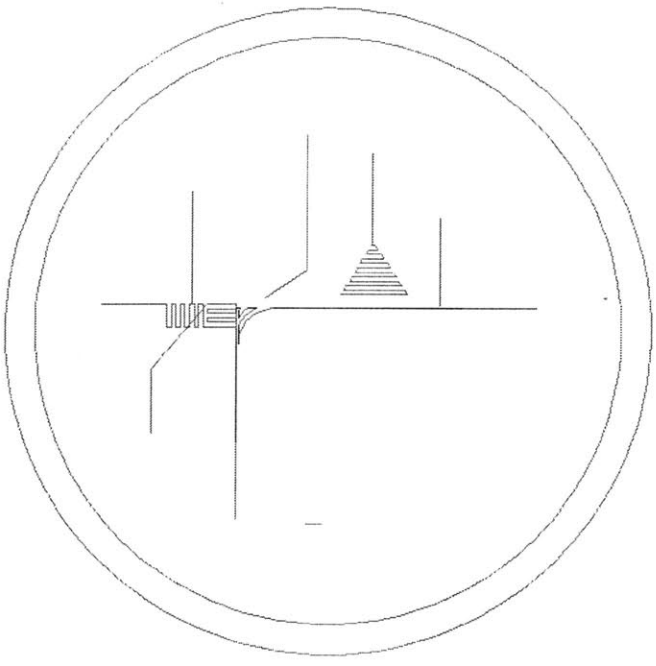

Main Channel:
Drill bit size: 1.5mm
Drill depth: 1mm

Control Channel/
Isolator/
Immobilizer:
Drill bit size: 1mm
Drill depth: .2mm

Figure 5 One of the mid-stage designs. Isolation chamber is the same as the design in Figure 4. However, the immobilization chamber has been modified in this version.

Since the early designs, there were many improvements on channel specifications and immobilization chamber. First, the channel width and depth were smaller to accommodate the size of zebrafish better. The control channels were made narrower and shallower to prevent zebrafish from getting stuck in the chip. Lastly, and most markedly, a different design was used for immobilization chamber. Instead of being trapezoidal, this one was rectangular. The left half of the chamber was deep enough to let the zebrafish's head through, but narrow enough for its tail to go through. The right half was milled in a slope that made the depth of the chamber as deep as the flow channel. With this mechanism, we were hoping that by applying suction from the left end of the chip, zebrafish's tail would be positioned in a consistent manner.

This design, however, posed new challenges. The immobilization chamber was too wide, causing the fish to get stuck at different places every time. In addition, due to the chamber's depth near the flow

channel, the depressive membrane on the fish was even less effective since the surface of the chamber that it was depressing on was not flat. You can see an attempt to immobilize a zebrafish in figure 6.

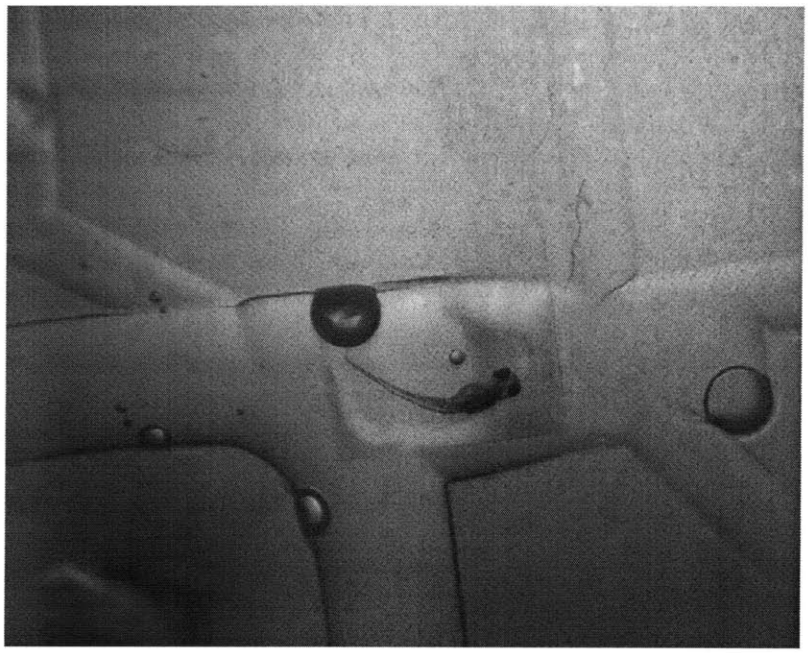

Figure 6 Zebrafish immobilized imperfectly in the chamber. Notice the depression layer not quite pressed on the right side near the fish's head. This chamber was also too large.

3.2.3 Last Stage Design

For this design, all the control channels were made even narrower and shallower by using .5mm-diameter drill bit. Also, the immobilization chamber was changed to employ a similar mechanism to the one in C Elegans chip designed by Zeng. The rectangular section was sloped so that the chamber got deeper as it got closer to the two separate control channels on the bottom. Although it is not visible through the 2-d Auto-cad plot, in G-code it was designed so that there is an extra room just big enough to fit one zebrafish. The mechanism in the design was to depress the immobilization depressive membrane to push the fish to the deeper side of the chamber, while supplementing the immobilization with the two suction channels. This is illustrated in figure 8. (The zebrafish used in the testing was older than 72hpf, which is why it does not fit in the room on the side)

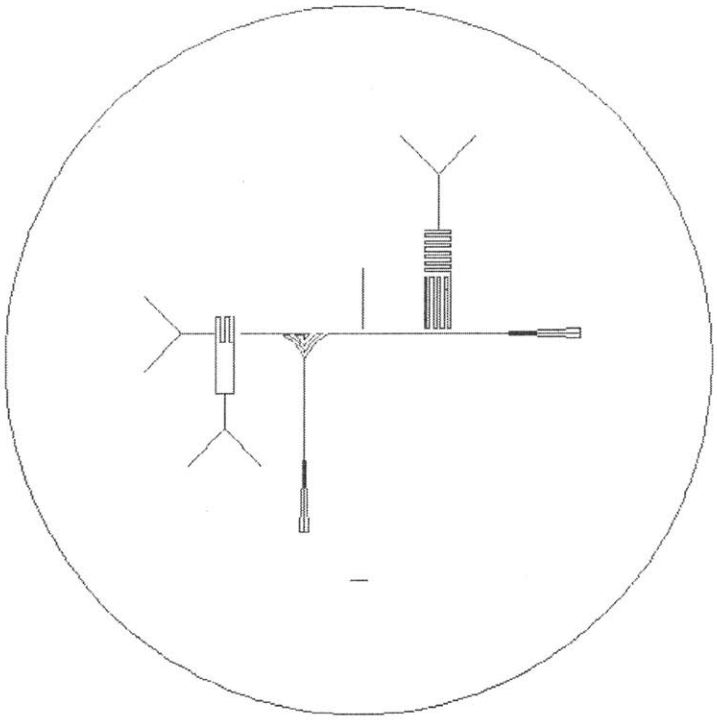

Main Channel:
Drill bit size: 1mm
Drill depth: 1mm

Control Channel/
Isolator/
Immobilizer:
Drill bit size: .5mm
Drill depth: .1mm

Figure 7 One of the late-stage designs. The immobilization chamber on the left is sloped towards the bottom of the chip. The inlet and outlet channels funnel out.

Input and output holes of the flow channel were also changed for this design. They get wider and deeper at the tip in order to diagonally insert 3mm-thick metal tubes to the chip. This diagonal insertion prevented zebrafish from hitting the bottom of the chip as they entered, thus reducing the mortality rate of zebrafish entering the chip.

After this stage of the design, using microfluidic chip to screen zebrafish was put on hold. The major reason was that there was no clear prospect of aligning zebrafish in a consistent manner, which was the basis of the entire project. Moreover the more iterations and experiments we tried manipulating zebrafish in microfluidic chips, the more we realize that using PDMS chips was not appropriate for the scale we were working with, which was more in millimeter scale than micrometer.

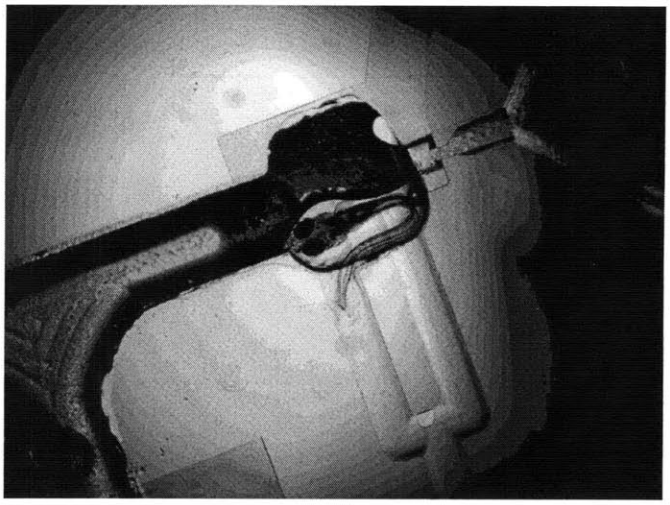

Figure 8 Zebrafish trapped in the immobilization chamber of chip design in figure 7. Zebrafish is trapped at the deeper part of the chamber after the immobilization layer depressed on it. The fish in this picture is older and bigger than the ones that are commonly used for screening, which is why it does not quite fit in the chamber.

4. Design of the High-throughput Screening Platform

There are largely two parts to this section: hardware and software components. The first section involves decisions and designs that shape the mechanical parts of the platform. The software interface of this system, which is in Matlab with a few components tested and supplemented in LabView, was partially adopted from the codes of Chris Rohde from C. Elegans group at the lab.

4.1 Hardware Components

The setup can be most easily described in order that zebrafish passes through it. Zebrafish is initially aspirated from a reservoir for mass screening, or manually from a Petri dish if there is a need to screen a select few animals. During the testing phase, a lot of the screening was done by aspirating the fish from Petri dish. Aspirated from the reservoir, the zebrafish passes through a photodetector unit which stops the flow once it recognizes a zebrafish. Afterwards, zebrafish is flown through the system at a slower pace until it gets under the microscope objective. At this stage, machine vision detects the fish through the signals from the camera, stopping the fish when it comes in view. After the fish is done with imaging under the objective, the zebrafish can be discarded, or dispensed and sorted in a multiwall plate. Figure 9 is the diagram of the prototype but it was not always the set-up that was used since most components were built and tested separately at points.

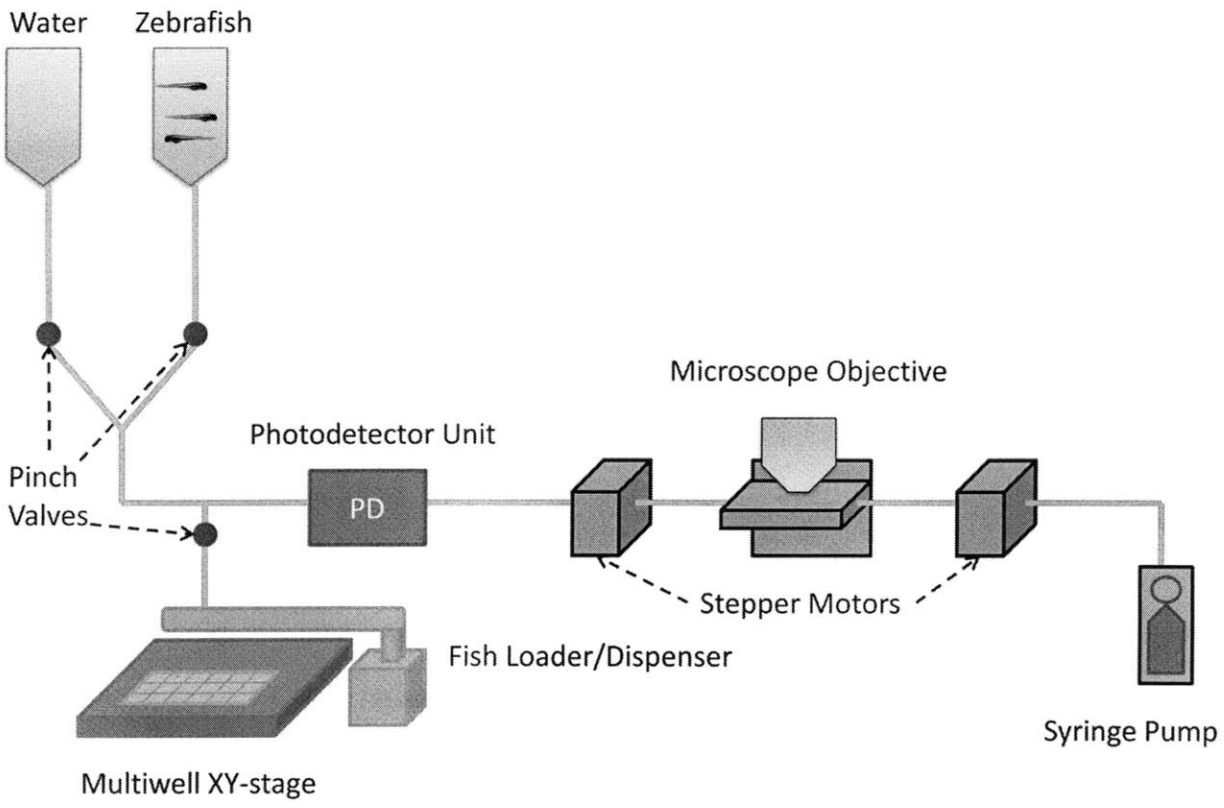

Figure 9 Schematic Diagram of the Platform

4.1.1 Photodetector Unit

a. Design Decisions

Building an automated high-throughput system meant a few things in the early stage of its design. One of the most important deliverables was an ability to automatically bring the fish under the objective. After speculation, the best two methods seemed to be using photodetector or using machine vision. Using the photodetector was successful in making the flow in the system stop when a fish entered the unit, but it was not so successful in transporting the fish right under the objective. This was because the distance that zebrafish travels in the tubes could not be controlled in a consistent manner even with a computer controlled syringe pump. The majority of the path that zebrafish passed through was made of

elastic silicon tube, which caused the ratio of distance traveled by zebrafish to amount of fluid aspirated by syringe pump fluctuate up to 15-20% at random.

One might ask why the photodetector system was not built right under the objective so that the zebrafish would be located right under the microscope when it's detected. This method posed two problems. First, due to the inherent delay caused by the time it takes for syringe pump to execute the signal sent from the program, the zebrafish always stopped past the photodetector unit. The elasticity of the tube contributed to this since it was observed that the fish still traveled through the tube by a centimeter or so after the syringe pump was stopped. Secondly, photodetector unit needed to be optically sealed in order to ensure that the photodetector did not detect other light sources in the laboratory or other parts of the system. Due to this physical constraint, it was not feasible to build the photodetector unit right under the objective even if there weren't the first problem.

Furthermore, even if this were not the case, it still would not have been efficient to just use photodetector as the sole mean of detecting and aligning the fish under the objective, because the alignment part will always require manual calibration of how much the syringe pump should aspirate for the fish to move from photodetector unit to the objective by trial and error. These two reasons led to using both the photodetector and machine vision for the platform.

The last question to be answered in this design was why not use only the machine vision instead of supplementing it with photodetector system that is not even that precise. The two reasons for this were the speed of the system and the need to isolate individual zebrafish in the screening process.

The first reason defeated the purpose of the platform of being high-throughput. From trial, we noticed that the machine vision can only detect the fish reliably at slower speed of the syringe pump between 100 and 200 Hz, whereas the photodetector could detect them at speed as high as 400/400. This was not an insurmountable amount of delay for the prototype, but it slowed down the basic functions of the platform by several seconds, which could double or triple the entire cycle duration. The

more crucial downside of running the system in slower speed throughout was that fish could actually swim away from the aspiration pressure at the bottom of the reservoir.

The second reason detracted from the reliability of the platform. If the flow was not stopped until the fish reached the objective, there was a high probability that there would be multiple zebrafish in the system already. By stirring the fish reservoir where the fish enters the system, we were able to reliably decrease the frequency of the fish entering the tubes and sufficiently increase the average distance between each fish that enters the platform, but not well enough to let one fish go through the distance to reach the area under the objective consistently without having another fish entering the platform. Having extra fish in the platform was not detrimental, but it did decrease the efficiency and the reliability significantly. First, the extra fish needed to be discarded, which should be avoided as much as possible. Secondly, the fish that entered the system at unexpected point could end up in the syringe pump at the end of the cycle which is highly advised against by the manufacturer due to the fact that there is no good way of cleaning the inside of the syringe. Thirdly, extra fish could remain at random points of the system, and those fish would soon turn into carcasses which clog up and contaminate the entire tube.

b. Photodetector Mechanism

The photodetector system needed to distinguish the signal of the fish passing through from the signals from air bubbles and water. We decided to have a green LED shine light through the capillary to the photodiode so when a bubble or a fish goes through, there would be perturbation to the output signal. The initial design only had one LED illuminating the capillary from the top, down to the photodiode. This was problematic because the negative peaks from air bubbles were larger than the ones from zebrafish. Therefore, we added a blue LED on the side to solve this problem. The blue LED light from the side was perpendicular to the light path of the green light, so the only light that entered the photodiode was the light scattered from the capillary. Since the air bubbles scattered more light than

zebrafish, the sum of two signals resulted in a larger peak for zebrafish. This manipulation enabled the photodetector system to bypass the peaks from the air bubbles and only detect the peaks caused by zebrafish passing through.

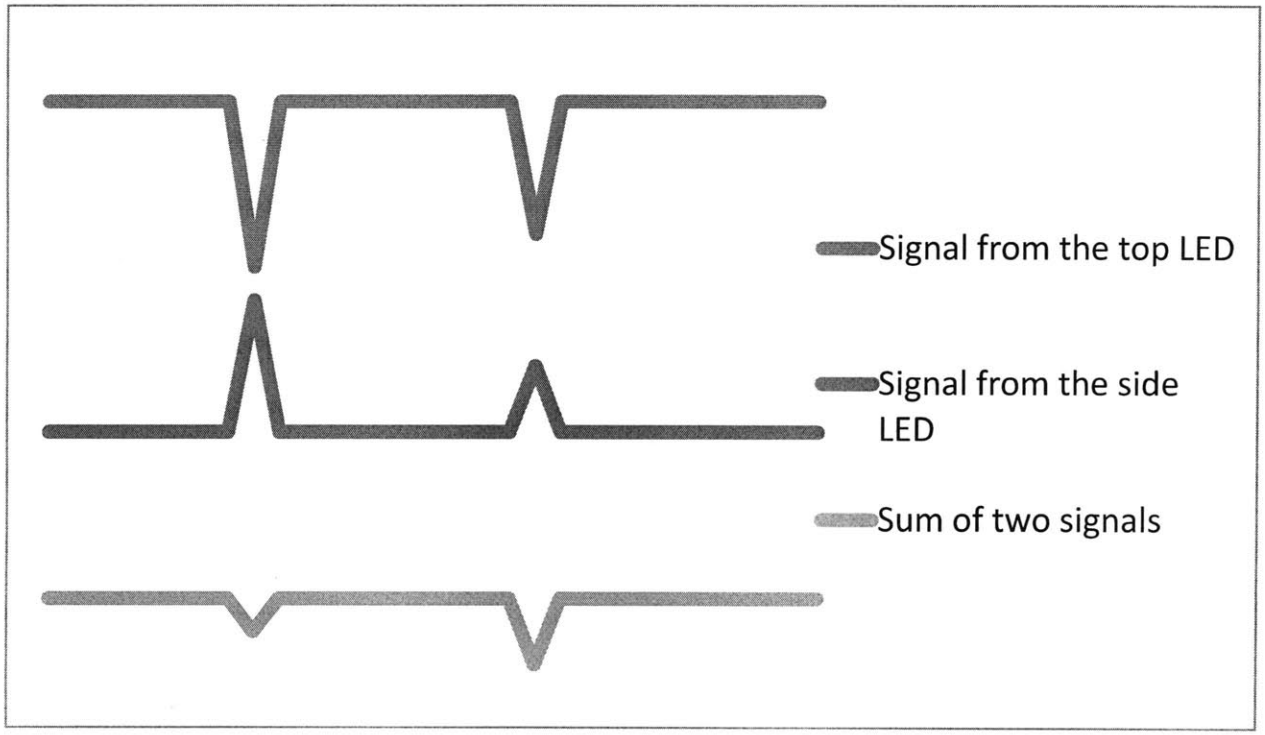

Figure 10 The Signal Logic for the Photodetector Unit. The first peak represents the signal from an air bubble, and the second peak represents the signal from a zebrafish. You see that with the two signals combined, zebrafish's signal has a bigger magnitude.

c. Design

i. Photodiode

Opt301 from Burr-Brown was used as the photodiode for the photodetector unit. OPT301 is an opto-electronic integrated circuit containing a photodiode and a transimpedance amplifier. The 0.09 x 0.09 inch photodiode is operated at zero bias for excellent linearity and low dark current. The

integrated combination of photodiode and transimpedance amplifier on the circuit prevents current leakage, high noise pick-up and gain peaking.[7]

This product was chosen for several reasons. First, it had the operating voltage range of 2.25 to 18V which sufficiently covered the ideal working voltage of 5V. It was one of the very few integrated circuit photodiode, which saved the effort of manually dealing with the internal impedance of the system. It was also packaged in a metal case that had through-hole extensions, which made it easier to integrate it and interface it with the Nidaq ports.

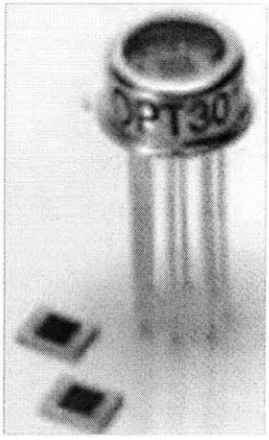

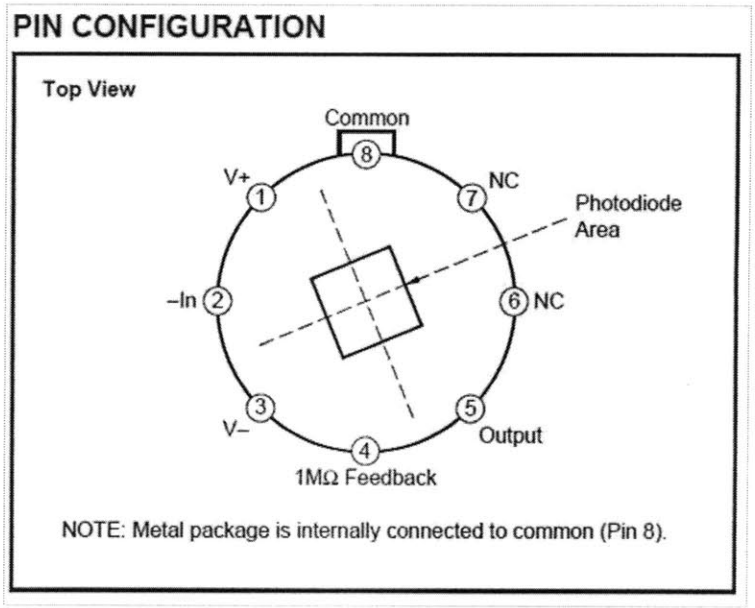

Figure 11 The picture (left) and the input/output diagram of OPT301 Photodiode Integrated Circuit

[7] Burr-Brown

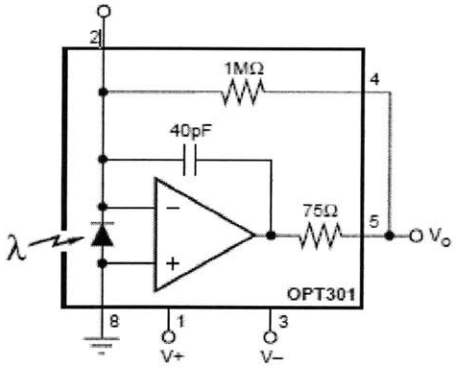

Figure 12 The inner circuitry of OPT301

ii. Photodetector Unit Circuit Design

The photodetector circuit includes the photodiode, a capacitor for reduced noise, and two solid state LED lamps. The circuit was built on a 1" X 1" breadboard with four wires from a rainbow cable: white wire for the output from the photodiode, red for the supply voltage of 5V, blue for the supply voltage of -5V, and black for ground. The figure outlines the circuitry around the photodiode.

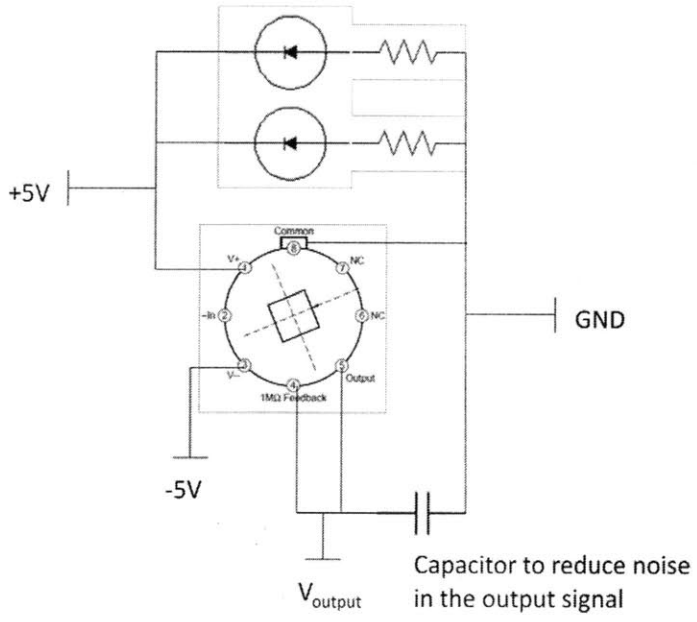

Figure 13 Circuit Design of the Photodetector unit. It is connected to four Nidaq ports. Note that the two LED's are integrated on the same board.

iii. Photodetector Unit Physical Design

In order to seal the unit from outside light, the entire system was enclosed in a plastic black box. To make sure that the light was concentrated on the capillary passing through the system without outside scattering, a block of Polyurethane was cut into a square piece with holes drilled through them so that the capillary goes through the center, while the photodiode was placed under and LED lamps on top and from the side perpendicularly, as seen in Figure 14.

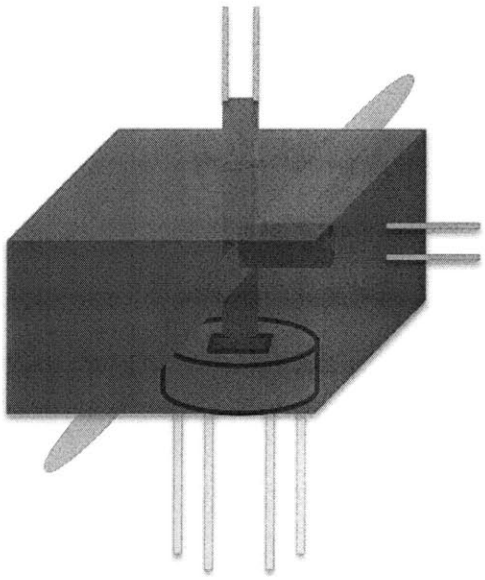

Figure 14 Diagram of Photodetector Unit. Green LED is shone right through the capillary on the photodiode, and the blue LED is shone perpendicular to the green light. Paths of light are all contained within the black polyurethane block

4.1.2 Objective Cage Unit

a. Design Decision

All the imaging for the platform was done with water immersion lenses. Water immersion technique enables a high-level magnification with less diffraction problem since the water's index of refraction is much closer to that of glass, which most lenses are made of. It also enables the objective to

immerse in the water that covers the cells, tissues, or organisms rather than having to image through a cover glass. For our platform, we needed to contain the Teflon tube in the water while being able to rotate the tube around during imaging. The tubes were fixed on shaft collars around stepper motors on both sides of the objective, which enabled computer-controlled rotation.

b. Teflon Tube Holder

The part that held the Teflon tube was built using a 1/8" thick polycarbonate plate. It was milled out into a square piece and with a rectangular area milled out with ledges around the boundary. In this milled out area, a .9inch by .4inch cover glass was placed with water-repellent grease on the edge to make it leak-proof. On both sides of the milled out area, a hole of 1/32" inch was drilled to let the Teflon tube pass through. This was one of the two parts of the platform that zebrafish passed through the Teflon tube rather than silicon tube, the other being inside the photodetector. Teflon was not flexible enough to be clamped down on the stepper motors on the sides or link to other tubes through Y-collar or capillary extensions.

c. Stepper Motors

One of the greatest appeals of the platform is that it can rotate the animal while screening. This is a crucial functionality since zebrafish, unlike C. Elegans, is a quite large and sophisticated. There are certain organs that are only visible at certain angles, so it is very important to be able to align the fish at least in the 3 perpendicular representative views: dorsal (top surface), ventral (bottom surface), and lateral (side surface).

The motors used in the cage set-up were stepper motors from Jameco. It had the step size of 1.8 degrees, which was more than precise enough for our usage. It was chosen also because it was light and small compared to its counterparts with similar power output. The supply voltage was 12VDC,

which was within the range of voltage that could be provided by the power source used in the lab. In order to secure the silicon tubes on the motors, a pair of motor shaft collars that can hold the tubes with socket set screws were built.[8]

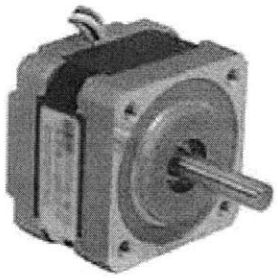

Figure 15 Photo of Jameco Stepper Motor

d. Motor Controllers

Most stepper motors, especially low-cost ones like the Jameco model, do not have built-in controllers or the necessary connections to interface with computers directly. They usually need motor drivers that can control it and even break down its step interval to smaller microsteps. The model used for this platform was Interinar BSD-02LH Step Motor Driver.

This model was chosen for many reasons. First, its inputs can be controlled by 10-pin rainbow cable, which makes the physical interface much simpler and organized than wiring every input individually. It can microstep at full-, half-, quarter-, and sixteenth- steps for any standard bipolar stepper motors. It operates at a current as high as 2.5A, and outputs up to 30V, which are both above the normal operating range for the Jameco motors.[9] It also has many safety features such as cross-current circuit protection, under-voltage lockout protection, and thermal lockout protection. It also possesses a very sizeable heat sink. These criteria are very important because the motor driver that was used with previous prototypes short-circuited often and overheated very rapidly while performing screening. BSD-02LH has not failed during screening besides from human errors.

[8] Jameco
[9] Interinar

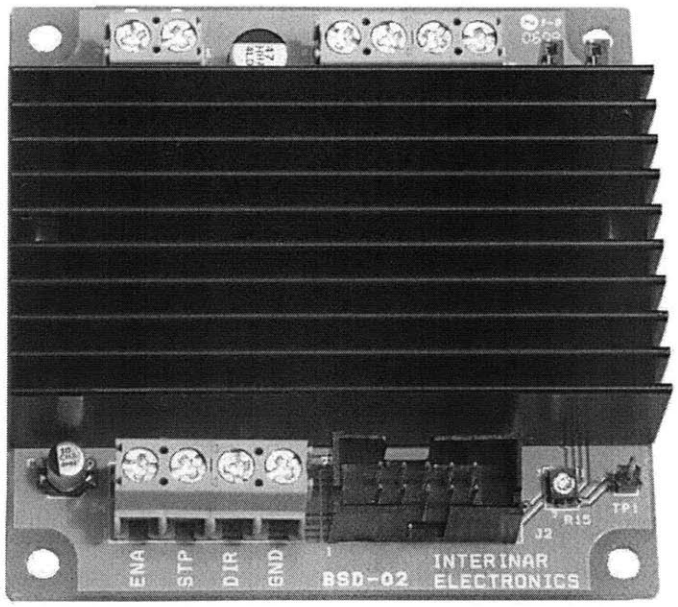

Figure 16 Photo of Interinar BSD-02LH Motor Controller. The black socket with ten gold pins is where a rainbow cable can be plugged in. However, the wires can also be connected individual through the green screw-in ports on bottome left and top left of the picture. The four ports on the top right are the ports where the four lead wires from bipolar stepper motor connects.

e. Cage

The physical cage itself was built with modified Thorlab parts and the two Jameco Motors. The motors were modified by putting two thread holes on two of the four holes on the back of the motor. Two solid aluminum plates were milled out with two paths that the motors could be secured with screws through the thread holes. These plates with the motors were held together by two foot-long posts. The entire cage was secured on XYZ stage system by the two posts.

4.1.2 Multiwell Plate Stage

a. Multiwell

In order to test a large library of assays on hundreds of fish, it is crucial to be able to organize them after screening. The most appropriate and standard container for this purpose is a 96-multiwell

plates. The individual wells in the multiwell this size has more than enough room for a fish to survive for a few days. For this project, round-bottom wells were used for the following reasons: The round bottom made it easier for syringe tips to aspirate zebrafish from the well, since there were no corners at the bottom.

As a matter of fact, zebrafish are small enough to fit in the wells of 384-multiwell plates. This switch, which will not involve much recalibration of the platform, can improve the system by four folds. However, there is a disadvantage in the health of zebrafish when raised in a smaller space. Ideally, the water in each reservoir of 96-well plate needs to be refilled daily to keep the living condition optimal. The wells in 384-multiwell plates are more than four folds smaller than the wells of 96-well plate, likely resulting in a living condition undesirable for long term growth. However, there was no noticeable difference between fish whose water have been refilled daily and the ones that have not been. There was no comparative health assessment done between zebrafish in a 96-well plate and a 384-well plate, but it should be considered in the future if the platform does adopt 384-well plates.

b. XY Stage

The multiwell plates were placed in a computer-controlled stage that could control its X-Y coordinate accurately. The initial model used for the project was Prior H101A. It was secured by four 6-inch Thorlab posts on the optical table to keep it immobile. The Prior stage actually overqualified for the purpose of directing the dispenser to the well, considering that the minimum step size for the Prior stage is 1 μm, and the distance between two adjacent wells in 96-well plate is 9mm.

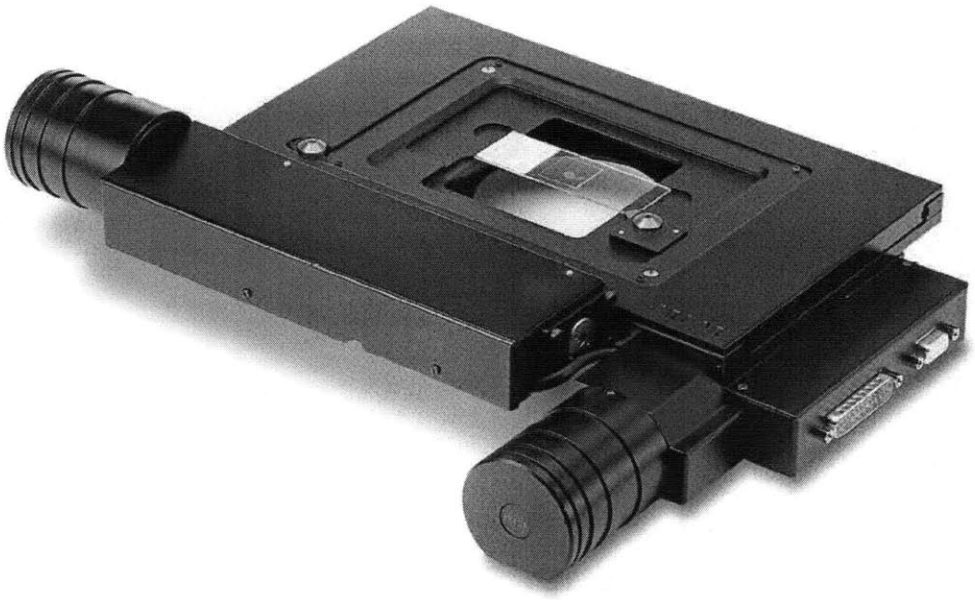

Figure 17 Photo of Prior H101A Stage.

c. Zebrafish Loader/Dispenser

The mechanism for getting the fish in and out of the capillary from the wells was not as straightforward as expected. Simply dipping the end of the Tygon silicon tubing was not a great strategy since silicon tube was too flaccid. Furthermore, it was discovered that aspiration of fish is more effective when the opening of the tube was wider, despite the fact that this decreased the pressure.

The design that resolved these issues was composed of two channels. We used a long metal syringe tips about 2 inches long that were secured by having them punctured through a PDMS block. The PDMS block also served as a sealer for the well that was being aspirated to ensure a more secure aspiration and prevent leakage. The inner pressure was balanced out by the second syringe tip that was connected to an open channel. The inner diameter of these tips was approximately three times as large as the Tygon tubing. The PDMS block with the syringe tips punctured through it was glued to a aluminum arm that was supported by a pneumatic actuator.

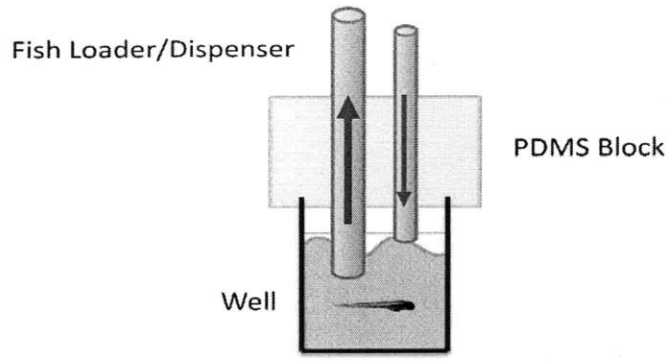

Figure 18 Diagram of Fish Loader/Dispenser in conjunction with one of the 96 wells on a plate. The narrower tip acts as an outlet to prevent pressure build-up during aspiration or dispensation

4.1.4 Syringe Pump

Syringe Pump plays a crucial role in this platform. It dictates the speed and acceleration of the flow in the tubing, which needs to be controlled and interfaced with practically all the other components in the platform such as the photodetector, pinch valves, and the camera. The product chosen for this task was Tricontinent C3000 model. We connected a 25ml syringe for our usage with minimum flow precision of 5µl. The device takes 24VDC, through three kinds of hardware interfaces: RS232, RS485, and CAN. For our platform, we interfaced the device to the computer through RS232. The syringe pump can be used to control 3 different flow connections with an adapter, but for this platform, only one connection was sufficient.

Figure 19 Photo of Tricontinent C3000
Precision Syringe Pump

4.1.5 Pinch Valves

The flow within the platform is relatively simple but it still involves fluid flowing in different directions for each steps. The apparatus we used to control these flows along with the syringe pumps were computer-controlled pinch valves. These pinch valves operate by pressing on the capillary on its high state, and releasing it in its low state. The product we chose was Biochem Valve model 075P2NC12-02SQ. The product operated on 12VDC, and the valve was fit for tubes with outer dimension between 1/16" and 1/8". Another important factor to consider while using pinch valves is the elasticity and adhesiveness of the capillary tubes. The silicone tube that was used for most of the channel in the platform was elastic enough that repeatedly applying pressure to stop the flow did not cause it to deform or stay stuck. However, when we tried Teflon PTFE and FEP with pinch valves, the capillary tubes were immediately damaged and bent.

Figure 21 Photo of Biochem-Valve
075P2NC12-02SQ Pinch Valve

4.2 Software Components

4.2.1 Syringe Pump Control

The Syringe pump is a central component of the platform outside of the parts involved with imaging. It controls the flow of the fluid inside the entire platform with accuracy of 5µl. [10] It needs to interface with the rest of the system at all times, especially with the photodetector and the camera.

There are three separate communication protocols that C3000 recognizes: OEM, DT, and CAN protocols. Since DT is designed to be used with a terminal emulator program with simpler syntax, DT was chosen for the Matlab Interface. In the DT protocol, a command can be inputted from the computer, but the syringe pump itself prints answer commands every time it performs an action. For this part of the project, we will focus only on the commands from the computer to the device.

[10] Tricontinent

a. DT Protocol

DT protocol operates in the following syntax:

1. The start character: ASCII symbol "/"

   The start character, which is always "/" in DT protocol, indicates the beginning of the message.

2. Pump Address

   The pump address indicates which channel on the adapter that the syringe pump would be sending or receiving a flow from. For this version of the platform, the syringe pump only had one channel connected to the system, with the other channel connected to a waste container. If pump address is missing in the command, the syringe assumes that the command is for the pump channel that it is currently set to.

3. Data Block

   This is the content of the command in ASCII. All commands must be followed by ASCII character "R" in order to run/execute.

4. End Character: Carriage Return [CR]

   End of the message is indicated by the carriage return, which can is standard on hyperterminal. In Matlab, the end character can be set by setting the terminator protocol as CR while establishing connection with the port.

b. Important C3000 Commands

There are dozens of C3000 software commands that can be used all across the three types of protocol. Not all commands manifest their feedback through physical motion from the pump. Some of the commands are only used to change settings such as speed and direction whereas some commands are used to report the status of the pump to the computer. Among them, the following essential

commands were used to run our high-throughput platform. Note that C3000 commands are case-sensitive.

i. Control Commands

R	Execute Command String
G<n>	Repeat command sequence n times (If n=0, the loop continues forever)
T	Terminate Command

ii. Initialization Command

Z<n>	Initialize plunger, emptying out the liquid in the syringe

We use n=0 for initialization, meaning that the plunger moves with full force during the process.

iii. Plunger Movement Commands

A<n>	Move plunger to absolute position, 3000 being the physical maximum of C3000
P<n>	relative pickup, meaning the plunger pulls fluid into the syringe
D<n>	relative dispense, meaning the plunger pushes fluid out of the syringe

For P and D, although the inputs are relative, if the syringe pump reaches either end of syringe's motion capacity, the motion will stop and it will print error message to the computer.

iii. Valve Commands

I	Move valve to input position
O	Move valve to output position

iv. Set Commands

v<n>	Set start velocity in Hz
V<n>	Set top velocity in Hz
c<n>	Set cutoff velocity in Hz

Hz that we use to describe plunger speed refers to half-step/second. The amount of liquid depends on the size of the syringe connected to the pump. As mentioned before, it can be as small as 5µl. The speeds set by the set command do not change until the pump is reinitialized by command [Z].

c. Command Input

All of these commands can be entered in a string as long as it is shorter than 255 characters, including the starting and ending character. For example, if the user wants to dispense 300 steps equivalent amount of liquid, he will input the following steps.

1. /1Z0R
2. /1v200V400c200R
3. /1ID300R

This will first initialize the pump, set the speed, and then dispense 300 full steps of liquid. Of course, the entire process could have been entered in a single string like the following:

/1Z0Rv200V400c200RID300R

If you want to keep aspirating fluid from the system, you can put a following command,

/1P5500OD5500G0R

This will repeat the IP2500OD2500 in a loop until the program crashes.

4.2.2 Motor Control

As described in the hardware component section of this thesis, the motor controller we used, BSD-02LH, receives 5V signals through a 10-pin rainbow cable that can be connected to the computer through a Nidaq card. Through the 10 pins as shown in figure, you can control how fast, how much, and in which direction the motor moves.

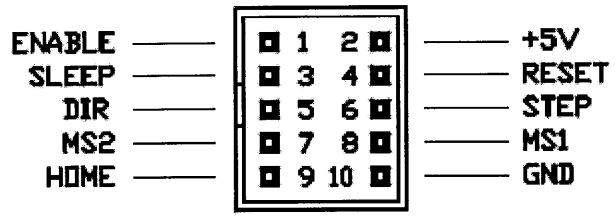

Figure 22 The diagram of the 10-pin connection of Interinar BSD-02LH Motor Controller

Pin #	Function	Description
1	Enable	When logic-high, disables the circuitry.
2	+5V DC	Unused.
3	Sleep	When logic-low, disables the circuitry. Opposite of Enable.
4	Reset	Unused.
5	Direction	Determines the direction of the rotation of the motor. Logic-high is for Counter clockwise rotation and logic-low is for clockwise rotation.
6	Step	A low to high transition advances the motor by one increment. Size of the increment is determined by MS1 and MS2
7	MS2	Determine the size of increment with MS1.
8	MS1	Determine the size of increment with MS2.
9	Home	Unused.
10	GND	Signal Ground.

Table 3 The functionalities of the 10-pin connection of the motor controller

Keeping the circuitry disconnected through "Enable" or "Sleep" signal is important in operating the motors, since they can overheat if the circuitry is constantly active. The motor needs to be used only briefly for less than a second since that is all it takes to align the fish, considering the maximum rotation that would be necessary for imaging is 180 degrees. In the earlier versions of the user interface, this part was overlooked and all the motors eventually got short circuited and even damaged a few BSD-02LH in the process. After integrating the "Sleep" signal in the user interface, the system has not failed.

MS1	MS2	Step Size
ON	ON	Full
ON	OFF	Half
OFF	ON	Quarter
OFF	OFF	1/16

Table 4 The microstep sizes based on the states of MS1 and MS2

Another important part to notice is the MS1 and MS2 pins that determine the step size of motor rotation. Depending on the on and off status of the two pins, the step motor's unit step size can be broken down into even fewer steps. BSD-02LH can break it down as low as 1/16 of the original size. This process is called microstepping. Microstepping is helpful in high precision environment since it makes it possible to rotate the object in a more precise angle, but also because smaller steps lessen the vibration caused from the movement. The Jameco motors that were used for the rotational unit had the step size of 1.8 degrees, which is already much more precise than what is desire for the platform. However, the decreased vibration and slower rotation provided more security on the capillary, which sometimes left the field of view after a rotation.

From Table 3, the minimum number of signals necessary to operate the motor is 5: Enable (or Sleep), Direction, Step, MS1, and MS2. In order to make the motor move one step, you input a low and a high in Matlab in a following way:

```
enable=0;
MS1=1;
MS2=1;
direction=0

data1= logical([enable direction 0 MS1 MS2]);
data2= logical([enable direction 1 MS1 MS2]);


putvalue(dio,data1);
putvalue(dio,data2);
```

First, you define the values for your static variables such as enable, MS1, MS2, and the direction, and then you set the two alternating logical data with first one with step value 0 and second with step value 1. Following that, you use the function "putvalue" to enter data1 and data2 back to back.

However, this only makes the motor move by one full step, which is 1.8 degrees. If you wanted to make the motor move in micro steps, you will have to account for the multiplicative factor depending on the value of MS1 and MS2. Therefore, in the final version of the Matlab function for the motor, the microstep variable was created along with the variable "steps" that calculates how many steps it would need for a given angle. The signal input will then be put in a for loop where it sends the signal "steps" many times:

```
microstepnumber=2^(MS1+2*MS2+MS1*MS2);
steps=round(Ang/1.8*microstepnumber);

for step=1:steps

    putvalue(dio,data1);
    putvalue(dio,data2);
end
```

4.2.3 Multiwell Stage Control

The software interface for the Prior Stage H101A used for the platform is called Pro Scan II. It is used to control not only the H101A, but multiple other stages and devices, some of which even have 3 dimensional controls. Similar to Tricontinent C3000, Prior H101A receives commands through RS232 port. Another thing it has in common is that the terminator type is <CR> just like C3000. It also possesses a large array of commands and other controls that enables a higher level control and interfacing with the Prior stage, but only the following few commands were necessary to operate the stage with the platform.

G, a, b, c	Move the stage a steps in x-direction, b steps in y-direction, and c steps in z-direction (not applicable for H101A)
P	Print the current position of the stage
I	Stop the stage

The syntax of Pro Scan is different from that of C3000. You do not need a start character. The content of the command is the first and last thing in the command, at least in the scope of this platform. Commands with numerical inputs need to be delineated by comma, space, tab, equals, semicolon, or colon. There can actually be multiple of these spaces or special characters. For the GUI, all the stage commands were separated by commas. It is also important to change the format of numerals into strings before sending it in the command. The numerical strings also have to be integers. The last notable big difference is that it is not allowed to append a series of different commands as you can in C3000. Each command must be entered separately and sequentially. This never became a problem since there was never a need to put conflicting commands to the multiwell stage.

G command moves the stage from its current position. It is a relative position command, not an absolute position. P command prints the current location of the stage. For the platform, the following two functions were used to detect the position of the stage and move accordingly.

```
function[readout] = goto_location(stage,x,y)

x = round(x);
y = round(y);
Sx = num2str(x);
Sy = num2str(y);

text = ['G,' Sx ',' Sy ',' 0];
fprintf(stage, text);


function[coords] = get_location(stage)

text = 'P';

fprintf(stage,text);

coords = fscanf(stage,'%s,%s,%s');
cords
```

4.2.4 Camera & Machine Vision

This part of the GUI was completely done by a teammate Carlos Pardo. This part of the system largely involved the detection and positioning of the fish in the field of view and also the capturing the

image of a zebrafish or taking a video of the screening process. The first part operates similarly to how the photodetector works. The difference is that with the camera, the field of view to collect pixel strength can be adjusted. This relieves the system of confusing bubbles with fish since it is only the boundaries of bubbles that block and scatter the light, whereas for zebrafish it is the entire body, especially the eyes. A signal threshold was set so that only when something dark and wide enough for the FOV passed through the capillary, the camera would recognize it as the fish. There is a possibility that a debris can be picked up, but as long as the fish are grown and transported in clean water, the probability is low.

4.2.5 Overall Control of the Platform

By implementing and interfacing with the respective parts of the platform, the graphic user interface for the system was developed. In this section, the order of the processes to run the platform will be described.

The default states of all the pinch valves are closed, and the microscope is illuminated by bright-field lighting. The process starts by running the "Initialize" on the syringe GUI. This initializes the syringe, making it ready to aspirate fluid. Afterward, run "Load" on the syringe GUI, which opens V1 and starts aspirating the fish and the fluid from the zebrafish reservoir. When a fish is detected in the photodetector, it shuts V1, opens V2, changes the aspiration speed to 200 from 400, and starts aspirating from the water tank instead of the zebrafish reservoir until the fish is detected under the microscope. Once the fish is detected, the light is switched to fluorescence from bright field. When the fish is positioned under the objective, one can use the controls on the Motor GUI to rotate the fish at the desired angle. Then image is captured using the given camera software. Afterwards, using the Multiwell GUI, one can select the well that the fish can be dispensed to by clicking on the respective well

and use the drop the piston command. Finally, the user can execute the unload command on the Syringe GUI, which shuts V2, opens V3, and dispenses the fish into the well.

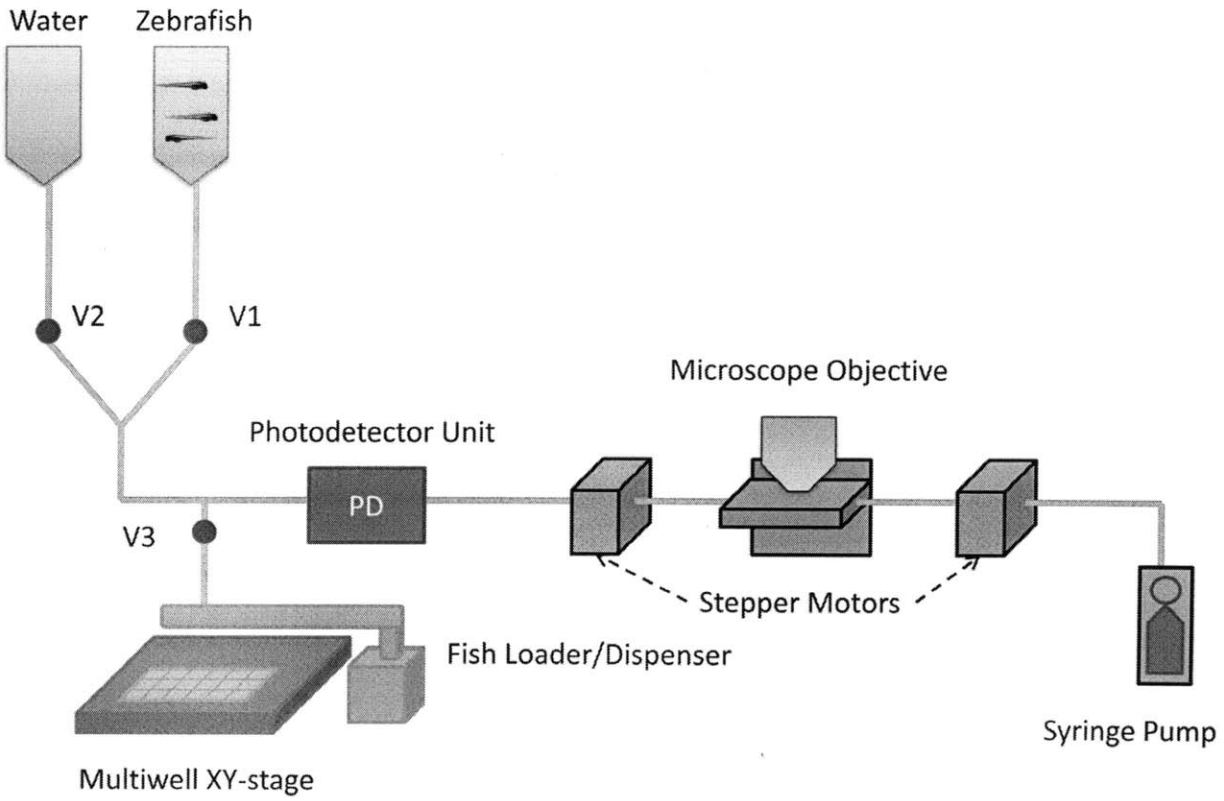

Figure 23 Schematic Diagram of the screening platform. V1,V2,V3 are the pinch valves that function as the logic gates of the screening process.

In case of platform malfunctioning, the Syringe GUI has a "stop" button, which stops the syringe pump. There is also a text box in the Syringe GUI that one can input explicit C3000 commands and execute by pressing on the "Manual" button in case there is a need to control the fluid outside of the conventional path necessary for the screening. "Fill with Water" command is physically opposite to initialize. It fills the syringe with water as opposed to emptying it. This is necessary when the syringe is pushed out empty but not all the fluid has made it out of the system yet. By bypassing the flow to the water supply and filling in the syringe, one can continue dispensing the fluid out without affecting the fluid flow inside the platform.

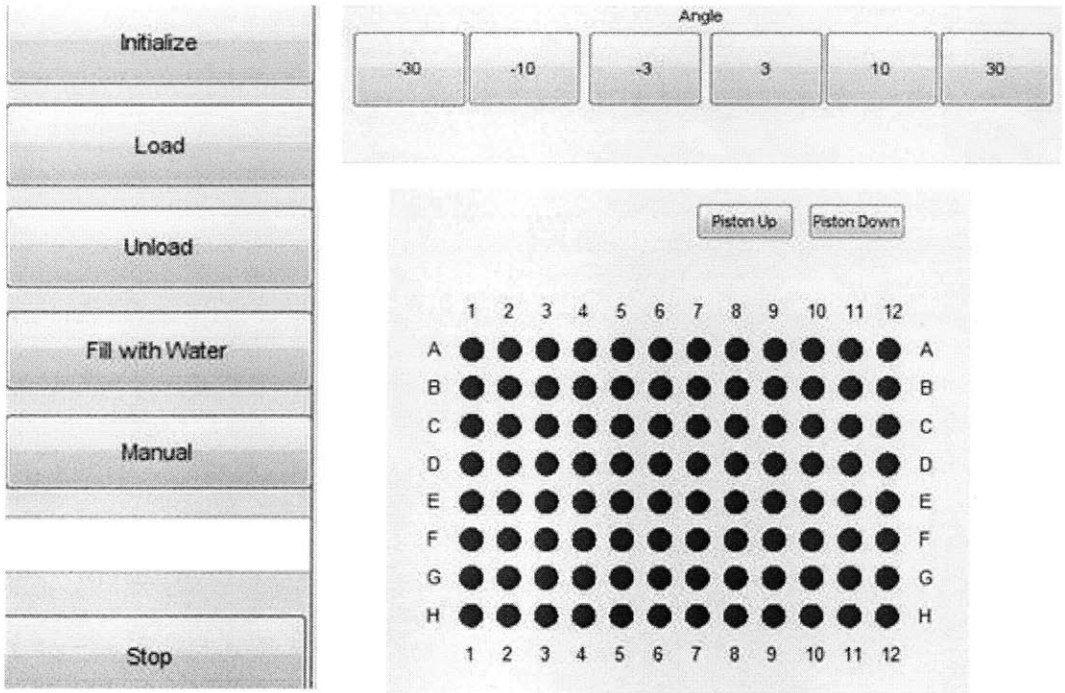

Figure 24 GUI for the screening platform. (Left) Syringe GUI (Right top) Motor GUI (Right bottom) Multiwell GUI

5. Platform Performance Testing

To measure and verify how well the platform works, two measurements were taken. First part was the health assessment of the zebrafish that went through the platform by observing the mortality rate, any physiological abnormality, and the time that the fish developed swimming bladder. Second part was measuring how long it took to run the zebrafish from one point of the platform to the next.

5.1 Health Assessment

There were two subparts to this assessment. First, we tested whether running the fish through the platform at a higher speed affected the fish's health. From this we could deduce how fast we can run the system within the limits of the syringe pump without damaging the fish.

Secondly, we wanted to determine how the circulation through the platform itself without any invasive or non invasive manipulation affects the zebrafish's health. If a large portion of the fish that went through the system died or developed swimming bladders late, it would indicate that the going through the platform indeed affected the health of zebrafish negatively.

5.1.1 Swimming Bladder

One of the most noticeable signs of zebrafish larva's health is the development of swimming bladders. They are a pair of semi-transparent sack-shaped organs that are farthest away from the back of the fish. These bladders develop later in the growth cycle or they do not develop at all, depending on how much the larva is damaged. There is no absolute timeline of when zebrafish is supposed to develop swimming bladders. Depending on factors such as the health of the parents and temperature, the pace of growth can vary by several hours. However, the embryos from the same parents grow at a similar pace because these factors affect them equally. Since swimming bladder was the easiest indicator of fish's health, we decided to record the time when we noticed the fully developed bladder for the first time to determine the difference between different control groups in terms of bladder growth.

Figure 25 Zebrafish with fully-developed swimming bladders (right) and with underdeveloped swimming bladders (left)

5.1.2 Assessment Method

For each series of assessments, zebrafish larvae from the same batch of crossing were used in order to ensure that there is no difference in maturity, environment, and hereditary genetics of individual fish. For the first part of the experiment, three sets of 32 fish were taken to test the system in three different speeds: 200/400/200, 300/400/300, and 400/400/400. The three numerical values refer to start speed, top speed, and cut-off speed in order. The reason that these three speeds were chosen was first because 200 provided enough force to aspirate the fish without it being able to swim away from the tip and 400 was the highest speed that the system could run.

The speed that was the fastest while retaining lowest mortality and abnormality rate was then determined to be the ideal speed of the system. For the second part, we took two sets of 50 fish to compare the fish that had gone through the platform on the ideal speed derived from the first part and the control group that had not.

Each group of fish was transported out of their original Petri dish into a smaller one and anesthetized with a Tricaine® 0.15mg/ml prior to entering the system. Fish were kept in anesthesia for the duration of the test to a maximum of 30 minutes. Once all of the zebrafish from the group went through the platform, they were moved to a container with clean water to wake them up from the anesthetized state. There suspected to be a minute amount of anesthetics that were transported with the fish themselves, but it did not seem to affect the result of the test. If it did, it affected both the

experiment and the control group. Once the fish were awoken in a new container, they were individually placed in a well of 96-multiwell plate.

After that point, the fish were observed every 4 hours for 16 hours, resulting in 5 reports including the initial state. In order to assess the health of the fish, the multiwall plate was observed with a microscope under bright-field light with maximum magnification of X5. Each fish was observed for the following traits: First, whether it was dead or alive. This was distinguished easily by the fact that dead fish turns opaque and starts rotting soon after its death. Supplementary step was to check if the heart was beating. Second criterion, which mostly affected the first round of observations, was whether there were any visible physiological abnormalities. Occasionally, the fish gets literally folded in half in the tube, which can permanently bend the body of the fish. Most prominent physiological abnormality observed during the experiment was a strain of edema. It did not cause any deaths from the data set, but it was clear that the fish with the condition suffered general arrhythmia and bradycardia. Edema also made the body more opaque, making it difficult to observe the development of swimming bladders. Lastly, and most importantly, it was noted on which round of the observation the swimming bladders were developed.

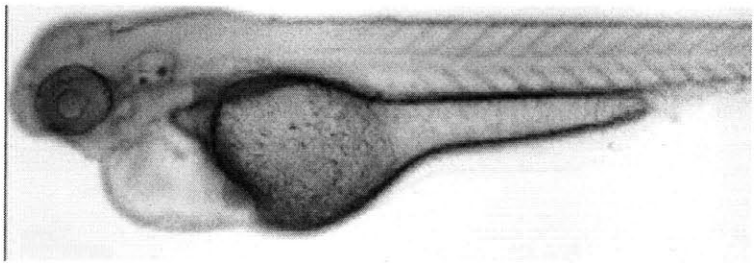

Figure 26 Zebrafish with edema. Internal organs, especially the yolk sack is more opaque and the chest cavity containing the heart is severely enlarged

5.1.3 Assessment Result

The first part of the test showed that there is little difference in the mortality rate within the three sets of speed that were tested. From the data set of 32 fish per trial, 96 fish total, there seemed to be no difference in the survivability or average swimming bladder development speed larger than the margin of error. There were a few more mortalities occurred in the first speed than second and third, with only one fish dying out of all three sets. The slight underperformance of 200/400/200, seemed to be caused by a few mistakes that were made while running the fish through the system. Since the slower speeds were tested first, I was not as adept or quick with the procedure, which could have likely caused more damage to the 200/400/200 group.

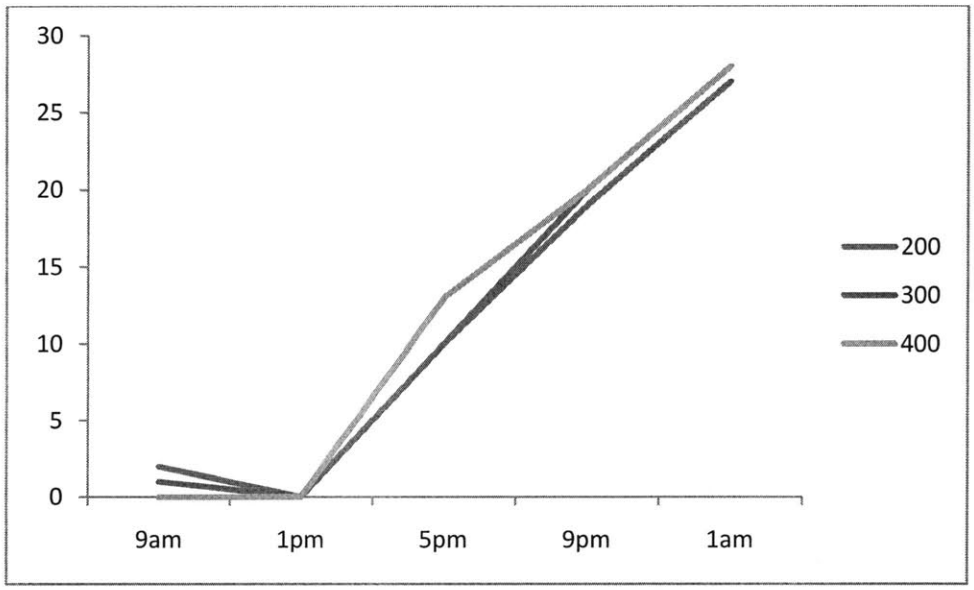

Figure 27 Number of zebrafish larvae with fully developed swimming bladders after going through the system at 200/400/200, 300/400/300, 400/400/400, respectively

The second part of the health assessment showed that the fish which went through the system developed swimming bladders later than the control group. However, this result was misleading since the edema that was described earlier in this section was displayed only in the group that went through the system.

Edema does not manifest itself as quickly as 30 minutes, and it was more likely caused by the environment or genetic sources. The eggs for this experiment were raised in two Petri dishes, which could have provided unknown environmental cause to affect some of the fish but not the other. All the fish with edema eventually developed swimming bladders like the normal ones, but it was a sign that edema slows down the growth and most likely the health of zebrafish larvae. Since there were total of 16 larvae with edema, 16 fish were taken out of the calculation and the graph was calibrated as if they had the same total, and the result was very close to each other as seen in figure 23. This result showed that running the fish through the system does not damage the fish enough to affect its mortality rate or growth of swimming bladders. From the first part, we can also infer that within the maximum speed range of the syringe pump, the zebrafish does not get hurt or benefit from a slower speed.

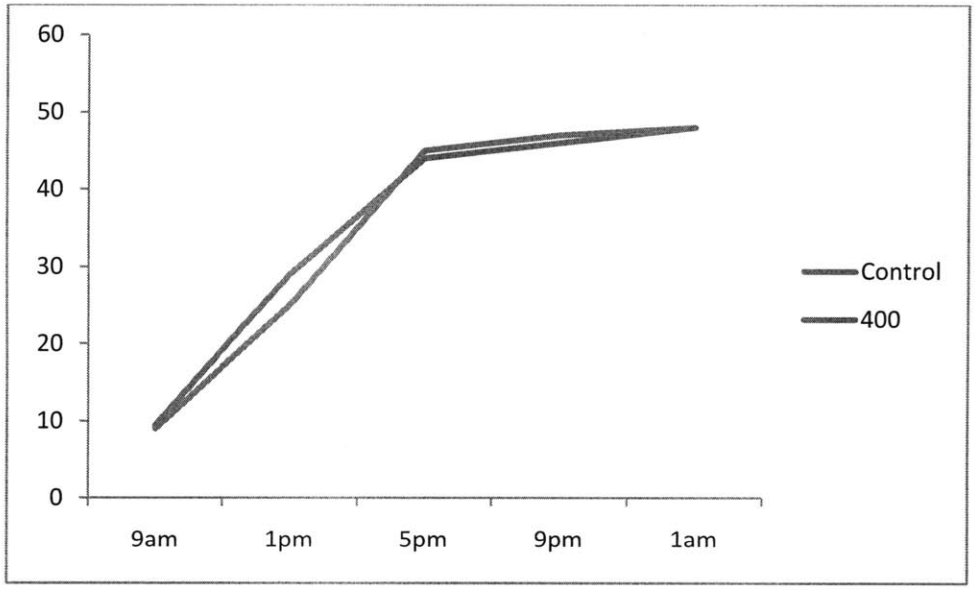

Figure 28 Number of zebrafish larvae with fully developed swimming bladders between the control group and the group that went through the system at 400/400/400 speed

5.2 Speed Measurement of Individual Parts of the System

The second part of the platform performance test dealt with the speed of the entire screening process. The initial goal of the project was to screen one zebrafish in less than twenty seconds. For this

project, it was possible to achieve an average screening time of 16 seconds, excluding the time it would take to take the image of the fish. Assuming that the image capturing process takes approximately 3-4 seconds, we achieved the initial goal in terms of time, which is nearly two orders of magnitudes smaller than an existing manual method of screening zebrafish involving individual imaging through microscope. Considering that the manual method is less robust, consistent, and accurate than using our platform, the progress we made on this project zebrafish screening technology is numerically and methodologically very significant.

5.2.1 Assessment Method

The test on the duration of screening was conducted on 150 fish on the five separate parts of the processes: 1. loading the fish from a reservoir up to the point where it is detected by the photodetector, 2. Moving the fish from photodetector to under the microscope 3. Bringing the fish into the field of view using the machine vision 4. Rotating and repositioning the fish 5. Dispensing the fish from the system. Each part was measured separately using a stop watch.

5.2.2 Assessment Result

Sections	Average Time	Standard Deviation
Reservoir to Detector	2.20	0.27
Detector to Microscope Stop	2.68	0.25
Tracking with the Microscope	2.92	0.60
Rotation and Reposition	5.62	1.69
Return Fish to Multiwell Plate	2.63	0.21
Total	15.68	1.75

Table 5 The average time spent per section of the platform and its standard deviation

The assessment test revealed that fluidic parts of the platform were robust and relatively consistent. Sections of the platform where there is little or no interaction between syringe pump and the rest of the system such as reservoir to detector, detector or microscope, and return fish to

multiwall plate, the average times were short and the standard deviations of the time were also within 10% of the of the actual time.

Tracking with microscope had the average time that was quite low and well within the reasonable range. However, the standard deviation was approximately twice as large as the previously-mentioned three sections. From observation, this seemed to be majorly due to the fact that fish don't always stop at the same spot when it is through the "detector to microscope stop" section. The standard deviation was still only 20% of the average time, which was within the reasonable bounds.

The rotation and reposition step, however, was inconsistent, not to mention the fact that it was the single slowest process among the five. There were several reasons for this problem. First, this was the only part of the platform where a user has to control the steps himself, naturally causing a lower consistency and higher standard of deviation. Secondly, it was revealed that the capillary was not aligned perfectly, causing it to shift horizontally while rotating. This problem added an extra step of "repositioning" the fish in order to bring the fish back in the field of view. Furthermore, especially if the fish were small and the capillary were rotated at a large increment, the inertia of the motion caused fish to keep rotating for 10-20 degrees or so after the motors stopped. Although this did not happen often, it required a couple smaller rotations to correct it.

The average of the total time summed over the five steps was 15.68, an astounding figure. This was certainly within the predicted range of the process. Considering the fact that the rotation and reposition problem can be solved by making a better capillary holder and possibly using an alternative capillary, possibly reducing 1 to 2 seconds from the total time, the platform could operate under 14 seconds besides the microscopy and laser surgery. The total screening time could then vary from 20 seconds to 30 seconds depending on how complicated or exacting the procedure needs to be, but for simple bright-field image capturing or even confocal imaging in the future, the average screening time per fish will certainly be within 20 seconds.

6. Imaging Capability of the Platform

This thesis focused mostly on the individual parts of the platform, their implementation, and optimization because it was the part of the platform that I was most involved with. However, the platform was not only efficient, fast, and largely automatic, but the imaging capability itself was of quality that could be extremely valuable to certain neurobiology research. It offers the ability to screen and image zebrafish in a way that was not available in the past. The following example is one of them.

Zebrafish with mutations on its astray gene displays a very distinct morphological abnormality in its retinal axons that can be imaged only from the dorsal view: When retinal axons navigate from the eyes to the brain, there are guidance molecules distributed along the optical pathway so that the axons grow to connect the brain and the eyes. However, when there are mutations on the astray gene, this axon guidance is severely compromised, causing the retinal axons to have excessive crossing with the axons from the other eye, and other general path-finding defects.[11] On a wild type fish, the retinal axons cross each other in an X-formation since left brain is connected to the right eye and vice versa. However, on astray fish, the retinal axons distribute randomly and cross over between left and right eyes. As seen in Figure 29, the screening platform successfully captured the retinal axon paths from the brain to the eyes for both cases. The visual difference between astray and wild type is so pronounced here that it would be possible to have the distinguishing process be automatic through machine vision process.

The astray mutation is just one example of how the screening platform with rotational capability can be utilized. We expect that there are more strains of zebrafish being researched in multiple fields that could take advantage of the imaging capability of our platform.

[11] Ficke

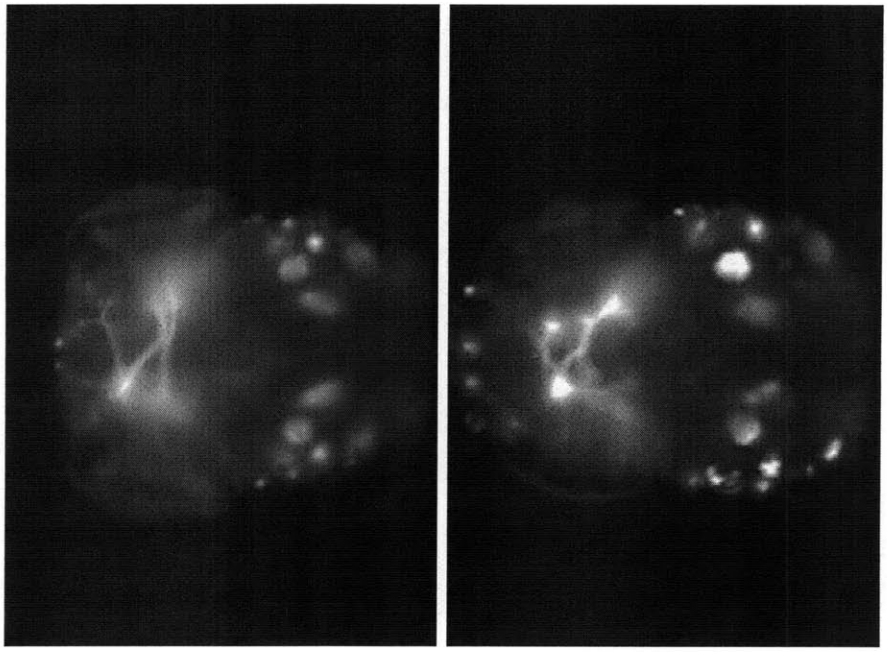

Figure 29 The images of wild type zebrafish (left) and astray zebrafish (right). The neuronal paths on the left form a clear X, whereas the ones on the right are randomly scattered from the brain to the eyes.

7. Future Work and Improvement

The work documented on this thesis is the progress that has been made in the high-throughput zebrafish screening platform up to January of 2010, when the first draft of *High-throughput subcellular-resolution in vivo vertebrate screening platform* was submitted to Nature Methods. The project continued and there have been several modifications and improvements made to the platform. In this section, those changes that have been made and the ones that will be made in the future are presented.

7.1 Confocal Imaging

It has been repeatedly pointed out that the toughest challenge in imaging zebrafish compared to C. elegans is the sheer size and the intricate composition of its body. The image quality is good as seen in Figure 29, but it is still not perfect. For instance, the wide-field fluorescence imaging, which was the method used to acquire images from the platform, leaves a lot of room for noise signals. This is helpful in a way when imaging organs that are not flat, such as the retinal neurons, which traverse different depth of fish's head in dorsal view. On the other hand, even in Figure 29, we can see that there is quite a bit of noise and background fluorescence that disrupt the axons we try to image. For the astray strain, the axons we tried to image themselves are distributed like tree roots, so it is not the clear neuron paths, but rather the chaotic spread that enable us to distinguish it from the wild type.

In the future iterations of the platform, confocal imaging will be used instead of the conventional wide-field fluorescence imaging. Confocal imaging is a technique patented by Marvin Minsky in 1957, which employs spatial pinhole to eliminate out-of-focus light and noise from the specimen that is thicker than the focal plane of the image. In conventional wide-field fluorescence microscopy, a light source illuminates the entire specimen, causing all parts of the specimen to be excited at the same time. This inevitably creates an excess of background fluorescence that end up making the image noisy. In contrast, confocal imaging uses a point illumination source in an optically conjugate plane to eliminate excitation of specimen that is not being focused on. This method only detects the image close to the focal plane

with much higher optical resolution. However, since most of the light is blocked in order to create point illumination, the signal intensity is much lower, which resultantly requires longer exposure.[12]

With confocal imaging, not only is it possible to get a better resolution on a single focal plane, but it can also scan multiple planes and combine them to create an image like the one in Figure 30, essentially mapping out all of the organs that are marked with fluorescence. It is also possible to use the same technique to create a 3-D image. The biggest challenge with these methods is the image acquisition time, but there are commercially available microscopes that employ different scanning methodologies to increase the frame rate of confocal imaging. Adopting confocal imaging techniques such as 3-D imaging is in the future plan of this project.

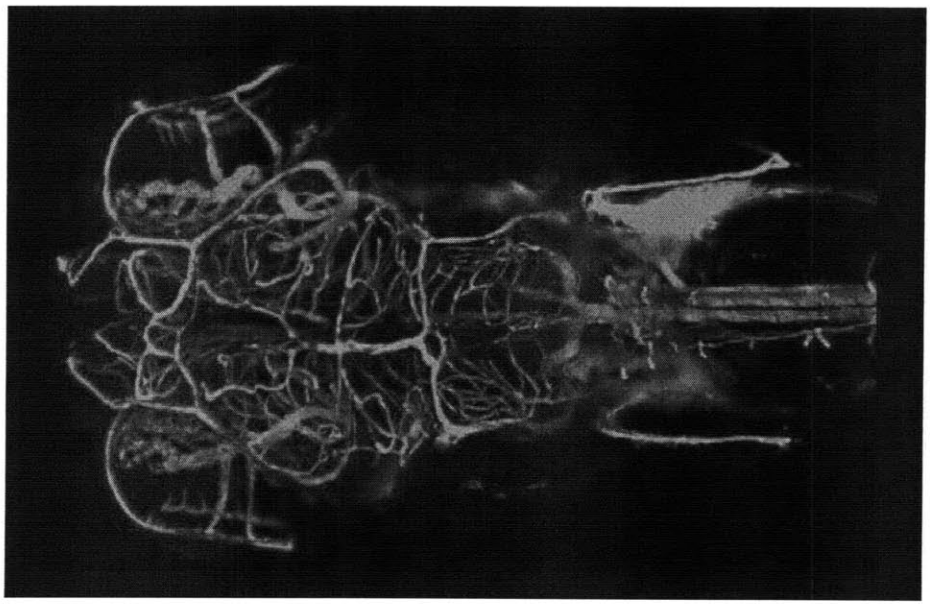

Figure 30 Digitally reconstructed image of confocal microscopic scans of zebrafish's head with fluorescence in its vasculature. (Weistein Laboratory, NIH)

[12] Pawley

7.2 Pipelined Screening

The old model of the platform operated on one syringe pump with a linear fluid flow from a fish reservoir to one multiwall plate, which was controlled by the Prior Stage. As described in the time assessment section, the duration of a screen was just below 16 seconds per fish. However, this number can be further decreased by operating the platform in parallel around the microscope. Understanding that the processes under the microscope such as laser surgery and imaging are the only ones that are limited by the resources, by adding more syringe pumps and modifying the fluid layout, the high-throughput system can be pipelined. The figure below shows a tentative schematic diagram of the pipelined system.

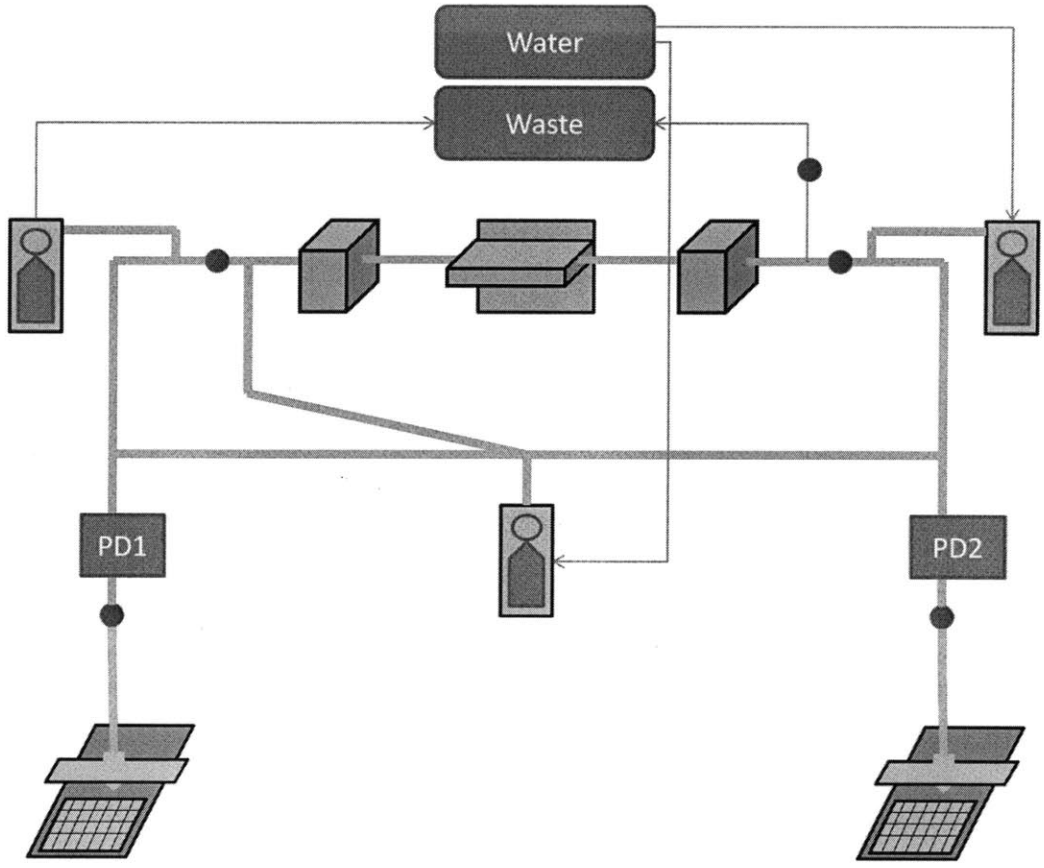

Figure 31 Tentative Schematic Diagram of the pipelined high-throughput screening platform. It operates with three syringe pumps and two multiwell plate stages.

A parallel set-up such as the one in Figure 31 enables the system to simultaneously aspirate fish and dispense them while a fish is being screened under the objective. Assuming that the five individual parts of the system function similarly to the one in the old model, the screening time can be decreased to the middle three steps, where the fish is moved from photodetector to microscope, tracked, and then rotated. Since the initial aspiration and dispensation processes are shorter than this series of three processes, the average screening time can be as low as 11.17 seconds without the imaging part. Once the rotation and reposition process is improved, which will be mentioned in the next section, the process can conceivably be under ten seconds per fish.

7.3 Ultrathin Borosilicate Capillary

The weakest link in the time assessment was the rotation and reposition step. The reposition should not even be necessary with well-calibrated calibrated capillary. However, with Teflon tube, which is inevitably flexible, and also with the capillary holder that was less accurate than desirable, the capillary was never aligned well enough to consistently stay in the FOV after rotation.

However, two changes were made in this part of the platform to improve stability of the capillary drastically. First, a different type of capillary was used in subsequent trials. A borosilicate capillary with thickness under 10μm was used instead of Teflon FEP. Although it was mentioned that glass has much higher index of refraction than Teflon, the ultrathin surface minimized the light scattering and it also had much less auto fluorescence due to its higher clarity. This glass capillary was narrower with an inner diameter of 600 μm which decreased the chance of zebrafish getting folded inside or jostling around during imaging. The second change was decreasing the length of the capillary holder, so there is less room for the capillary to be misaligned. The entry points on the sides were also drilled with a smaller drill bit, which made the capillary fit better. The resulting capillary holder and glass capillary combination did not move under the objective after rotation at all. The exact time assessment for the new model has not been done, but it is estimated to be less than 3 seconds now.

8. Summary

The main objective of this project was to develop an automatic high-throughput zebrafish screening platform that can perform a screen at a rate faster than 20 seconds per fish. While there are still many areas to improve and add functionalities to, the initial goal was achieved by the point this thesis was written. The capability and the robustness of the platform were demonstrated by the health assessment, time assessment, and trial screenings of strains such as astray mutation.

The initial effort to emulate Zeng and Rohde's methods used for C. elegans proved to be ineffective, but that is not to say that microfluidic chip cannot be integrated in the future iterations of the platform. Some of the design decisions that came to replace the microfluidic chips, such as the idea of imaging zebrafish inside a capillary, and being able to rotate them using step motors were not the most quantitatively challenging or technically exacting. However, they were central to distinguishing this platform and project from the previous efforts in the field.

The development of the stable platform depended heavily on the choice of devices to be integrated such as the Prior stage H101A , Tricontinent C3000 syringe pump, Jamesco step motors, Interinar BSD-02LH motor controllers, and Burr-Brown OPT301 photodiode. Physically designing and modifying thse devices were non-trivial tasks and interfacing them through Matlab involved creating a carefully laid out integrated GUI that could handle all the inputs simultaneously. On top of these, the fact that the devices and the platform were constantly dealing with live animals and fluid made the development and optimization process even more difficult.

It should be noted that the high-throughput platform, which has already demonstrated its utility and robustness, has much more room for growth and diversification by pipelining and integrating a confocal microscope. This platform truly has an unfathomable value in how much it can advance and accelerate the current progress in the field of high-throughput neurobiology.

9. Bibliography

BRUCE A. BARUT AND LEONARD I. ZON "Realizing the potential of zebrafish as a model for human disease" Division of Hematology/Oncology, Children's Hospital, Department of Medicine, 2000

BURR-BROWN CORPORATION "OPT 301 Integrated Photodiode and Amplifier Manual" Texas Instruments, USA, 1994

PETER D. CURRIE AND GRAHAM J. LIESCHKE "Animal models of human disease: zebrafish swim into view" Nature Review| Genetics, Volume 8, May 2008

CORNELIA FRICKE, JEONG-SOO LEE, SILKE GEIGER-RUDOLPH, FRIEDRICH BONHOEFFER, CHI-BIN CHIEN "Astray, a Zebrafish roundabout Homolog Required for Retinal Axon Guidance" Department of Neurobiology and Anatomy, University of Utah Medical Center, Science 292 (5516):507-510, 2001

ANETTE FUNFAK, ANDREAS BROSING MICHAEL BRAND, AND JOHANN MICHAEL KOHLER "Micro fluid segment technique for screening and development studies on Danio rerio embryos" The Royal Society of Chemistry, June 2007

INTERINAR ELECTRONICS "Functional description of BSD-02LH Module"

CHARLES B. KIMMEL, WILLIAM W. BALLARD, SETH R. KIMMEL, BONNIE ULLMANN, THOMAS F. SCHILLING "Stages of Embryonic Development of the Zebrafish" Institute of Neuroscience, University of Oregon,; Department of Biology, Dartmouth College , 1995

PAWLEY JB "Handbook of Biological Confocal Microscopy (3rd Edition)" Berlin, 2006

TRICONTINENT SCIENTIFIC, INC. "C3000 Precision Pump Software Manual" 2010

W.H. WANG, X.Y. LIU, Y. SUN "Autonomous Zebrafish Embryo Injection Using a Microrobotic System" Advanced Micro and Nanosystems Laboratory, University of Toronto, Canada, September 2007

FEI ZENG, CHRISTOPHER B. ROHDE, AND MEHMET FATIH YANIK "Sub-cellular precision on-chip small-animal immobilization, multi-photon imaging and femtosecond-laser manipulation imaging and femtosecond-laser manipulation" Research Laboratory of Electrical Engineering, Massachusetts Institute of Technology, April 2008